Journal of Sound and Vibration 499 (2021) 115991

Contents lists available at ScienceDirect

Journal of Sound and Vibration

journal homepage: www.elsevier.com/locate/jsv

Component replacement TPA: A transmissibility-based structural modification method for in-situ transfer path analysis

J.W.R. Meggitt[a,*], A.S. Elliott[a], A.T. Moorhouse[a], A. Jalibert[b], G. Franks[c]

[a] Acoustics Research Centre, University of Salford, Greater Manchester, M5 4WT, UK
[b] Bentley Motors Ltd., Pyms Lane, Crewe, CW1 3PL, UK
[c] Hottinger Brüel & Kjær Engineering Services, Millbrook, Bedfordshire, MK45 2YT, UK

ARTICLE INFO

Article history:
Received 7 September 2020
Revised 26 January 2021
Accepted 28 January 2021
Available online 30 January 2021

Keywords:
Transfer path analysis
Structural modification
Component characterisation
Blocked forces
Transmissibility

ABSTRACT

In-situ transfer path analysis is a diagnostic method used to analyse the propagation of noise and vibration through complex built-up structures. Its defining feature is the independent characterisation of an assembly's active components (i.e. vibration sources) by their blocked forces. This independent characterisation enables the downstream structural modification of an assembly without affecting the sources' operational characteristics. In practical engineering structures, however, there is often a need to alter or replace components that reside *within* a vibration source, for example resilient mounts. An upstream structural modification of this sort would alter the blocked force and thus invalidate any response predictions made thereafter. Hence, an alternative approach is required. In the present paper a transmissibility-based structural modification method is introduced. We derive a set of equations that relate the blocked force and forward transfer functions obtained from an initial assembly, to those of an *upstream modified* assembly. Exact formulations are provided, together with first and zeroth order approximations for resiliently coupled structures. These component replacement expressions are verified by numerical examples.

1. Introduction

Transfer Path Analysis (TPA) is a diagnostic method used for analysing the propagation of noise and vibration in complex built-up structures, for example, vehicles, buildings, ships, etc. It has become an essential tool in the development and refinement of structures whose vibro-acoustic response is of interest. There exist many variants of TPA, differing in their implementation and interpretation [1,2]. Popular variants include classical [3], in-situ [4], component-based [5], operational [6,7] and transmissibility-based [8,9] TPA. In the present paper we are concerned with the variant known widely as in-situ TPA (also as blocked force TPA) [4].

* Corresponding author.
E-mail address: j.w.r.meggitt1@salford.ac.uk (J.W.R. Meggitt).

https://doi.org/10.1016/j.jsv.2021.115991

In an in-situ TPA the active components of an assembly (i.e. vibration sources) are each characterised by their blocked force; the force required to constrain their interface degrees of freedom (DoFs) such that their velocity (also displacement and acceleration) is zero. The blocked force independently describes the operational activity of a vibration source; it does not depend on what the source is connected to. This is advantageous as it means that the blocked force can be used in conjunction with structural modification techniques, where the receiver structure is modified in some way, for example in a design optimisation context [10–12].

Once characterised, the contribution of each active component to an operational response is determined using transfer functions measured between the source-receiver interface and the chosen target DoF. Based on their relative contributions, an engineer is able to identify troublesome vibration sources/transmission paths and investigate appropriate design changes.

Application of in-situ TPA requires the definition of a source-receiver interface; this interface implicitly defines what is considered as the 'source' of vibration. The source-receiver interface is, however, somewhat arbitrary, and is typically chosen for convenience rather than to satisfy some physical distinction. As a practical example, vibration isolators are often included as part of a source definition (i.e. the source-receiver interface is defined as being that between the isolator and the receiver, as opposed to the source and the isolator). Although this interface is perfectly admissible, it does place a limitation on what structural modifications can be investigated.

In contrast to a downstream structural modification, an upstream modification will alter the source definition, and thus invalidate any response predictions made in the modified assembly. We are interested in extending the possibility of structural modification upstream, such that a sub-component of a vibration source may be modified or replaced. For example, we may wish to alter the resilient coupling that has been included as part of a source definition. To achieve an upstream modification of this sort, its influence on the blocked force and forward transfer function, obtained from some initial assembly, must be predicted. In the present paper we introduce a transmissibility-based structural modification to do so. Its application provides the modified blocked force and forward transfer function, according to a known component replacement, and thus enables response predictions to be made in the modified assembly without requiring re-characterisation of the blocked force.

Having intoduced the context of this paper, its remainder will be organised as follows. Section 2 will begin by briefly introducing in-situ TPA, before Section 3 describes the proposed Component Replacement TPA (CR-TPA) method; Section 3.1 will derive expressions for the modified blocked force, and Section 3.2 for the modified forward transfer function. A summary of the key equations is given in Section 3.3. Two numerical validation studies will be provided in Section 4 before Section 5 draws some concluding remarks.

2. In-situ transfer path analysis

In-situ transfer path analysis aims to identify the dominant sources of vibration that contribute to a particular response (e.g. the sound pressure level in a vehicle cabin) by first characterising their operational activity, and then the transfer paths through which they contribute. In-situ TPA differs from classical TPA in that the source activity is characterised *independently* using the blocked force, as opposed to the contact force (which depends on the dynamics of the receiver structure).

In an in-situ TPA the blocked force is obtained using the inverse relation [13],

$$\tilde{\mathbf{f}}_c^S = \left(\mathbf{Y}_{bc}^C\right)^{-1}\mathbf{v}_b \tag{1}$$

where, with reference to Fig. 1a: $\mathbf{v}_b$ is an operational velocity measured on the coupled assembly at the indicator DoFs b; $\mathbf{Y}_{bc}^C$ is the mobility matrix of the *coupled* assembly C, measured between the indicator and interface DoFs, b and c, respectively; and $\tilde{\mathbf{f}}_c^S$ is the sought-after blocked force. Note that the interface DoFs c may be considered a subset of the indicator DoFs b. If the number of indicator DoFs is greater than interface DoFs, $|b| > |c|$, the matrix inverse may be interpreted as a pseudo-inverse. Implementation of Eq. (1) requires a two part measurement procedure. In part 1, the source is turned off and the mobility matrix $\mathbf{Y}_{bc}^C$ is measured. In part 2, the source is operated and the velocity $\mathbf{v}_b$ is measured.

Once the blocked force has been obtained it can be used to predict the operational response at some target DoFs r in the assembly. This forward response prediction is given by,

$$\begin{pmatrix}\mathbf{p}_r\\ \hline \mathbf{v}_r\end{pmatrix} = \begin{bmatrix}\mathbf{H}_{rc}^C\\ \hline \mathbf{Y}_{rc}^C\end{bmatrix}\tilde{\mathbf{f}}_c^S \tag{2}$$

where: $\mathbf{p}_r$ and $\mathbf{v}_r$ are operational pressure and velocity predictions; $\mathbf{H}_{rc}^C$ and $\mathbf{Y}_{rc}^C$ are the vibro-acoustic transfer function and transfer mobility, respectively, between the interface and target DoFs, c and r; and $\tilde{\mathbf{f}}_c^S$ is the acquired blocked force from Eq. (1). Together, Eqs (1) and (2) constitute what is known as in-situ/blocked force TPA.

Note that the blocked force is an independent, or invariant, source property (hence the superscript S); it can be used to predict the operational response in *any* assembly, provided that its coupled transfer functions are known. In the more general case, where $\mathbf{H}_{rc}^C$ or $\mathbf{Y}_{rc}^C$ are predicted using dynamic sub-structuring, for example, the above is typically referred to as component-based TPA [1].

In the present paper we are interested in Eqs (1) and (2) in the presence of an upstream assembly modification. This issue will be discussed further in the following section.

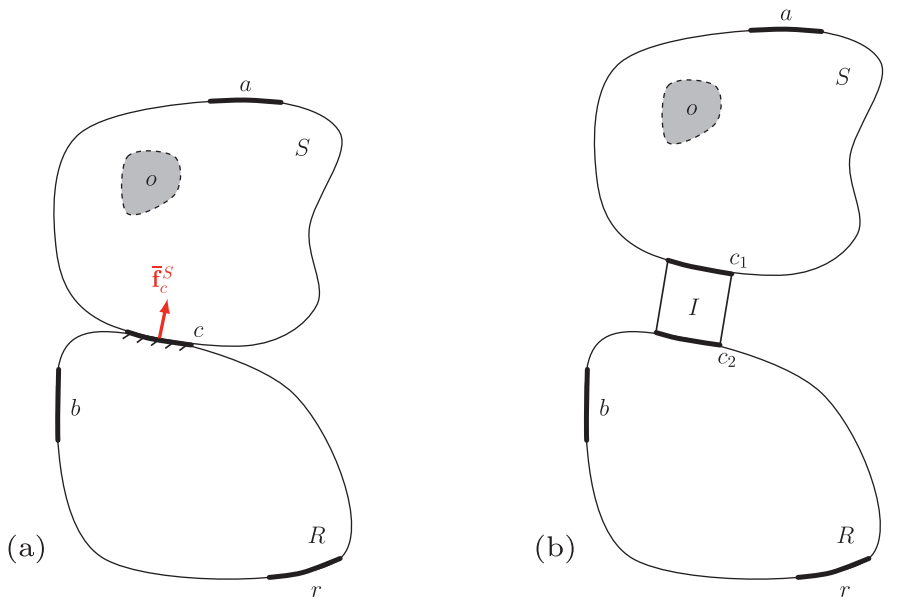

Fig. 1. Diagrams of general assemblies; (a) - Source-Receiver assembly, (b) - Source-Mount-Receiver assembly. Labels take the following meaning: *a* - remote source side DoFs, *b* - receiver side 'indicator' DoFs, *r* - remote target DoFs, *o* - internal source DoFs where operational forces act (assumed inaccessible), *c* - interface DoFs, c_1 - primary interface DoFs, and c_2 - secondary interface DoFs.

3. Component replacement transfer path analysis

Often when performing an in-situ TPA, access to the preferred source-receiver interface is limited and the required measurements cannot be undertaken. In this case, it is possible to redefine the source-receiver interface elsewhere, typically further downstream, i.e. into the receiver structure. By doing so, we redefine the source and receiver to include and exclude the appropriate components. Take for example the source-mount-receiver assembly in Fig. 1b. Although the interface c_1 may be the preferred choice, as it is the natural source interface, the interface c_2 may equally be considered. In this case, the source definition is set to *include* the mount, which is now excluded from the receiver.

Whilst the definition of source and receiver is somewhat arbitrary, if we wish to investigate the effect of replacing or modifying a component it must be located downstream of the defined source-receiver interface (i.e. within the receiver structure). Only then can standard structural modification methods be used. Any modifications made upstream of the source-receiver interface will affect the source definition, and in turn alter the blocked force. For example, suppose the mount in Fig. 1b were replaced by some other coupling; the blocked force at the interface c_2 would be modified accordingly. When performing an in-situ TPA one must also consider the forward transfer function between the defined source-receiver interface and the chosen target DoFs. Clearly, the modification or replacement of any upstream component will also influence this transfer function.

In the present paper we are interested in the replacement (or modification) of the upstream component $I_1 \rightarrow I_2$. We wish to predict its effect on the blocked force $\bar{\mathbf{f}}_{c_2}^{SI}$, the forward transfer function $\mathbf{Y}_{rc_2}^{C}$ (or $\mathbf{H}_{rc_2}^{C}$), and consequently the target response $\mathbf{v}_r$ (or $\mathbf{p}_r$). Hence, we are interested in the structural modifications,

$$\bar{\mathbf{f}}_{c_2}^{SI_1} \quad \xrightarrow{?} \quad \bar{\mathbf{f}}_{c_2}^{SI_2} \tag{3}$$

$$\mathbf{Y}_{rc_2}^{C_1} \quad \xrightarrow{?} \quad \mathbf{Y}_{rc_2}^{C_2} \tag{4}$$

where superscripts 1 and 2 denote the initial and modified assemblies, respectively. To achieve the above we propose a novel transmissibility-based structural modification method, Component Replacement TPA (CR-TPA).

With reference to Fig. 1b, CR-TPA requires that a primary interface c_1 is defined. Any component modifications *must* take place downstream of this primary interface. The blocked force $\bar{\mathbf{f}}_{c_2}^{SI}$, defined at some secondary interface c_2, is related to the primary interface blocked force $\bar{\mathbf{f}}_{c_1}^{S}$ via a blocked force transmissibility, which takes into account the properties of the initial assembly. This primary interface blocked force will be independent of any modifications made upstream of the secondary interface, so long as they remain downstream of the primary interface. Using a second blocked force transmissibility, based on the modified assembly, a modified blocked force at the secondary interface can be obtained. A similar procedure is used to obtain the modified forward transfer function.

The modified blocked force and forward transfer function equations will be derived in Sections 3.1 and 3.2, respectively, and summarised in Section 3.3. Section 4 will then present a numerical demonstration of the proposed CR-TPA.

Although not the primary concern of this paper, based on developments presented below, Appendix A derives a *downstream* transmissibility-based modification. That is, the replacement of a constituent component in the receiver structure when the primary interface c_1 is considered.

3.1. Modified blocked force

Shown in Fig. 1b is an assembly whose source is excited externally (or internally) at some DoF a (or o). FFrom the perspective of the receiver structure, this excitation can be represented by an equivalent excitation at the primary interface c_1, corresponding to the negative blocked force [13,14]. Hence, the equations of motion of this assembly, in mobility form, are given by,

$$\begin{pmatrix} \mathbf{v}_{c_1} \\ \mathbf{v}_{c_2} \\ \mathbf{v}_r \end{pmatrix} = \begin{bmatrix} \mathbf{Y}^C_{c_1c_1} & \mathbf{Y}^C_{c_1c_2} & \mathbf{Y}^C_{c_1r} \\ \mathbf{Y}^C_{c_2c_1} & \mathbf{Y}^C_{c_2c_2} & \mathbf{Y}^C_{c_2r} \\ \mathbf{Y}^C_{rc_1} & \mathbf{Y}^C_{rc_2} & \mathbf{Y}^C_{rr} \end{bmatrix} \begin{pmatrix} -\bar{\mathbf{f}}^S_{c_1} \\ \mathbf{0} \\ \mathbf{0} \end{pmatrix}. \tag{5}$$

In impedance form, we have equivalently,

$$\begin{pmatrix} -\bar{\mathbf{f}}^S_{c_1} \\ \mathbf{0} \\ \mathbf{0} \end{pmatrix} = \begin{bmatrix} \mathbf{Z}^{SI}_{c_1c_1} & \mathbf{Z}^{I}_{c_1c_2} & \mathbf{0} \\ \mathbf{Z}^{I}_{c_2c_1} & \mathbf{Z}^{IR}_{c_2c_2} & \mathbf{Z}^{R}_{c_2r} \\ \mathbf{0} & \mathbf{Z}^{R}_{rc_2} & \mathbf{Z}^{R}_{rr} \end{bmatrix} \begin{pmatrix} \mathbf{v}_{c_1} \\ \mathbf{v}_{c_2} \\ \mathbf{v}_r \end{pmatrix}. \tag{6}$$

Note that whilst the mobility terms of Eq. (5) characterise the assembly C as a whole, the impedance terms above characterise individual components (S, I, R), or couplings thereof (SI, IR).

By applying an appropriate blocking force at the secondary interface c_2, we are able to enforce the constraint $\mathbf{v}_{c_2} = \mathbf{0}$ (and consequently $\mathbf{v}_r = \mathbf{0}$),

$$\begin{pmatrix} -\bar{\mathbf{f}}^S_{c_1} \\ \bar{\mathbf{f}}^{SI}_{c_2} \\ \mathbf{0} \end{pmatrix} = \begin{bmatrix} \mathbf{Z}^{SI}_{c_1c_1} & \mathbf{Z}^{I}_{c_1c_2} & \mathbf{0} \\ \mathbf{Z}^{I}_{c_2c_1} & \mathbf{Z}^{IR}_{c_2c_2} & \mathbf{Z}^{R}_{c_2r} \\ \mathbf{0} & \mathbf{Z}^{R}_{rc_2} & \mathbf{Z}^{R}_{rr} \end{bmatrix} \begin{pmatrix} \mathbf{v}_{c_1} \\ \mathbf{0} \\ \mathbf{0} \end{pmatrix}. \tag{7}$$

From the top row of Eq. (7) we obtain,

$$\mathbf{v}_{c_1} = -\left(\mathbf{Z}^{SI}_{c_1c_1}\right)^{-1} \bar{\mathbf{f}}^S_{c_1} \tag{8}$$

which upon substitution into the second row yields,

$$\bar{\mathbf{f}}^{SI}_{c_2} = -\mathbf{Z}^{I}_{c_2c_1}\left(\mathbf{Z}^{SI}_{c_1c_1}\right)^{-1} \bar{\mathbf{f}}^S_{c_1}. \tag{9}$$

Eq. (9) relates the primary and secondary interface blocked forces (due to an excitation at a or o), through what may be interpreted as a blocked force transmissibility,

$$\bar{\mathbf{T}}^a_{c_2c_1} = -\mathbf{Z}^{I}_{c_2c_1}\left(\mathbf{Z}^{SI}_{c_1c_1}\right)^{-1} \tag{10}$$

where the over-bar $\bar{\square}$ is used to denote a *blocked force* transmissibility, as opposed to a velocity transmissibility, for example. Note that the primary interface blocked force, $\bar{\mathbf{f}}^S_{c_1}$, is by definition independent of the components I and R, whilst the secondary interface blocked force, $\bar{\mathbf{f}}^{SI}_{c_2}$, is independent of only the receiver component R.

By considering the inverse of the above we can formulate an equivalent expression that relates the secondary interface blocked force to that of the primary,

$$\bar{\mathbf{f}}^S_{c_1} = -\mathbf{Z}^{SI}_{c_1c_1}\left(\mathbf{Z}^{I}_{c_2c_1}\right)^{-1} \bar{\mathbf{f}}^{SI}_{c_2}. \tag{11}$$

Suppose we obtain a secondary interface blocked force, $\bar{\mathbf{f}}^{SI_1}_{c_2}$, from some initial assembly with the component I_1 installed. From Eq. (11), we can obtain the primary interface blocked force $\bar{\mathbf{f}}^S_{c_1}$. Then, using Eq. (9) for an assembly with component I_2 installed, we can obtain the modified blocked force $\bar{\mathbf{f}}^{SI_2}_{c_2}$. All together we have that,

$$\bar{\mathbf{f}}^{SI_2}_{c_2} = \mathbf{Z}^{I_2}_{c_2c_1}\left(\mathbf{Z}^{SI_2}_{c_1c_1}\right)^{-1} \mathbf{Z}^{SI_1}_{c_1c_1}\left(\mathbf{Z}^{I_1}_{c_2c_1}\right)^{-1} \bar{\mathbf{f}}^{SI_1}_{c_2} \tag{12}$$

where the superscripts 1 and 2 are used to denote the initial and modified assemblies, respectively. Eq. (12) provides an exact modification of the blocked force $\bar{\mathbf{f}}^{SI}_{c_2}$, due to the component replacement $I_1 \rightarrow I_2$.

Note that Eq. (12) has been formulated in terms of component impedances. An analogous expression can be derived in terms of assembly mobilities as follows. The velocity response at the secondary interface c_2, due to an excitation at a (or o), may be reproduced exactly by the application of an appropriate blocked force at either c_1 or c_2,

$$\mathbf{v}_{c_2} = \mathbf{Y}^C_{c_2a}\mathbf{f}_a = -\mathbf{Y}^C_{c_2c_1}\bar{\mathbf{f}}^S_{c_1} = -\mathbf{Y}^C_{c_2c_2}\bar{\mathbf{f}}^{SI}_{c_2}. \tag{13}$$

Pre-multiplication of Eq. (13) by the inverse mobility matrix $\left(\mathbf{Y}^{C}_{c_2c_1}\right)^{-1}$ then yields,

$$\tilde{\mathbf{f}}^{S}_{c_1} = \left(\mathbf{Y}^{C}_{c_2c_1}\right)^{-1}\mathbf{Y}^{C}_{c_2c_2}\tilde{\mathbf{f}}^{SI}_{c_2} \tag{14}$$

from which we can identify the blocked force transmissibility as,

$$\tilde{\mathbf{T}}^{a}_{c_1c_2} = \left(\mathbf{Y}^{C}_{c_2c_1}\right)^{-1}\mathbf{Y}^{C}_{c_2c_2} = -\mathbf{Z}^{SI}_{c_1c_1}\left(\mathbf{Z}^{I}_{c_2c_1}\right)^{-1}. \tag{15}$$

From Eq. (15) a mobility-based analogue of Eq. (12) can be formulated as,

$$\tilde{\mathbf{f}}^{SI_2}_{c_1} = \left(\mathbf{Y}^{C_2}_{c_2c_2}\right)^{-1}\mathbf{Y}^{C_2}_{c_2c_1}\left(\mathbf{Y}^{C_1}_{c_2c_1}\right)^{-1}\mathbf{Y}^{C_1}_{c_2c_2}\tilde{\mathbf{f}}^{SI_1}_{c_2}. \tag{16}$$

Given that we are interested in the component replacement $I_1 \rightarrow I_2$, the impedance form of Eq. (12) will prove more convenient in what follows. Substituting an impedance summation for the coupled *SI* impedance, $\mathbf{Z}^{SI}_{c_1c_1} = \mathbf{Z}^{S}_{c_1c_1} + \mathbf{Z}^{I}_{c_1c_1}$, Eq. (12) may be rewritten as,

$$\tilde{\mathbf{f}}^{SI_2}_{c_2} = \mathbf{Z}^{I_2}_{c_2c_1}\left(\mathbf{Z}^{S}_{c_1c_1} + \mathbf{Z}^{I_2}_{c_1c_1}\right)^{-1}\left(\mathbf{Z}^{S}_{c_1c_1} + \mathbf{Z}^{I_1}_{c_1c_1}\right)\left(\mathbf{Z}^{I_1}_{c_2c_1}\right)^{-1}\tilde{\mathbf{f}}^{SI_1}_{c_2} \tag{17}$$

where it is noted that the source impedance is unchanged between the two assemblies. Substitution of the source impedance for the free source mobility, $\mathbf{Z}^{S}_{c_1c_1} = \left(\mathbf{Y}^{S}_{c_1c_1}\right)^{-1}$, then yields,

$$\tilde{\mathbf{f}}^{SI_2}_{c_2} = \mathbf{Z}^{I_2}_{c_2c_1}\left(\left(\mathbf{Y}^{S}_{c_1c_1}\right)^{-1} + \mathbf{Z}^{I_2}_{c_1c_1}\right)^{-1}\left(\left(\mathbf{Y}^{S}_{c_1c_1}\right)^{-1} + \mathbf{Z}^{I_1}_{c_1c_1}\right)\left(\mathbf{Z}^{I_1}_{c_2c_1}\right)^{-1}\tilde{\mathbf{f}}^{SI_1}_{c_2}. \tag{18}$$

Eq. (18) provides an exact modification of the blocked force, requiring the point and transfer impedance of the coupling elements I_1 and I_2, and the free source mobility. Eq. (18) may be rewritten to avoid the free source mobility by addition and subtraction of the initial coupling element point impedance within the leftmost matrix inversion,

$$\tilde{\mathbf{f}}^{SI_2}_{c_2} = \mathbf{Z}^{I_2}_{c_2c_1}\left(\mathbf{Z}^{S}_{c_1c_1} + \mathbf{Z}^{I_2}_{c_1c_1} + \mathbf{Z}^{I_1}_{c_1c_1} - \mathbf{Z}^{I_1}_{c_1c_1}\right)^{-1}\left(\mathbf{Z}^{S}_{c_1c_1} + \mathbf{Z}^{I_1}_{c_1c_1}\right)\left(\mathbf{Z}^{I_1}_{c_2c_1}\right)^{-1}\tilde{\mathbf{f}}^{SI_1}_{c_2},$$

which simplifies to,

$$\tilde{\mathbf{f}}^{SI_2}_{c_2} = \mathbf{Z}^{I_2}_{c_2c_1}\left(\mathbf{Z}^{SI_1}_{c_1c_1} + \left[\mathbf{Z}^{I_2}_{c_1c_1} - \mathbf{Z}^{I_1}_{c_1c_1}\right]\right)^{-1}\mathbf{Z}^{SI_1}_{c_1c_1}\left(\mathbf{Z}^{I_1}_{c_2c_1}\right)^{-1}\tilde{\mathbf{f}}^{SI_1}_{c_2}. \tag{19}$$

Unlike Eq. (18), which required the free source mobility, Eq. (19) requires the coupled impedance of the initial *SI* assembly, $\mathbf{Z}^{SI_1}_{c_1c_1}$. This is available experimentally if excitations can be performed at both the primary and secondary interface. By measuring the coupling element's interface mobility matrix, the impedance $\mathbf{Z}^{SI_1}_{c_1c_1}$ can be obtained by matrix inversion as [15],

$$\begin{bmatrix} \mathbf{Z}^{SI}_{c_1c_1} & \mathbf{Z}^{I}_{c_1c_2} \\ \mathbf{Z}^{I}_{c_2c_1} & \mathbf{Z}^{IR}_{c_2c_2} \end{bmatrix} = \begin{bmatrix} \mathbf{Y}^{C}_{c_1c_1} & \mathbf{Y}^{C}_{c_1c_2} \\ \mathbf{Y}^{C}_{c_2c_1} & \mathbf{Y}^{C}_{c_2c_2} \end{bmatrix}^{-1}. \tag{20}$$

Note however, if the above measurement were possible, then one would likely define the blocked force at the primary interface to begin with. Nevertheless, Eqs. (19) and (20) provide an exact modification of the blocked force that avoids the need for the free source mobility.

If only response measurements are available at the primary interface (i.e. no excitations can be made) it is possible to use an indirect approach to obtain the necessary impedance $\mathbf{Z}^{SI}_{c_1c_1}$. Recall the impedance and mobility-based transmissibility relation (Eq. (15)),

$$-\mathbf{Z}^{SI}_{c_1c_1}\left(\mathbf{Z}^{I}_{c_2c_1}\right)^{-1} = \left(\mathbf{Y}^{C}_{c_2c_1}\right)^{-1}\mathbf{Y}^{C}_{c_2c_2}. \tag{21}$$

Post-multiplication by the coupling element transfer impedance yields,

$$\mathbf{Z}^{SI}_{c_1c_1} = -\left(\mathbf{Y}^{C}_{c_2c_1}\right)^{-1}\mathbf{Y}^{C}_{c_2c_2}\mathbf{Z}^{I}_{c_2c_1}. \tag{22}$$

By using the reciprocity relation $\left(\mathbf{Y}^{C}_{c_2c_1}\right)^{-1} = \left(\mathbf{Y}^{C}_{c_1c_2}\right)^{-\mathrm{T}}$, we arrive at,

$$\mathbf{Z}^{SI}_{c_1c_1} = -\left(\mathbf{Y}^{C}_{c_1c_2}\right)^{-\mathrm{T}}\mathbf{Y}^{C}_{c_2c_2}\mathbf{Z}^{I}_{c_2c_1} \tag{23}$$

which provides an indirect estimate of the *SI* assembly impedance $\mathbf{Z}^{SI}_{c_1c_1}$, based on the coupled mobilities $\mathbf{Y}^{C}_{c_1c_2}$ and $\mathbf{Y}^{C}_{c_2c_2}$, and the assumed known transfer impedance $\mathbf{Z}^{I}_{c_2c_1}$. Noting that $\mathbf{Z}^{SI}_{c_1c_1} = \mathbf{Z}^{S}_{c_1c_1} + \mathbf{Z}^{I}_{c_1c_1}$, the source impedance can also be obtained indirectly as per,

$$\mathbf{Z}^{S}_{c_1c_1} = -\left(\mathbf{Y}^{C}_{c_1c_2}\right)^{-\mathrm{T}}\mathbf{Y}^{C}_{c_2c_2}\mathbf{Z}^{I}_{c_2c_1} - \mathbf{Z}^{I}_{c_1c_1}. \tag{24}$$

Note that the measurement of $\mathbf{Y}^{C}_{c_1c_2}$ requires a response measurement at the primary interface. If this is not possible we are unable to provide an exact modification of the blocked force. In the special case that the coupling element being replaced constitutes some form of isolation (e.g. a resilient coupling), we can assume an impedance mismatch between

the source and coupling element, and some progress can be made. Mathematically, we can express this assumption in the following form,

$$\mathbf{Z}^{SI}_{c_1c_1} = \mathbf{Z}^{S}_{c_1c_1} + \kappa\,\mathbf{\Lambda}^{I}_{c_1c_1} \tag{25}$$

where: $\mathbf{Z}^{I}_{c_1c_1} = \kappa\,\mathbf{\Lambda}^{I}_{c_1c_1}$ is the coupling element point impedance, κ is some small numerical constant, and $\mathbf{\Lambda}^{I}_{c_1c_1}$ is an appropriate unscaled matrix. Providing that $\kappa\,\mathbf{\Lambda}^{I}_{c_1c_1}$ is sufficiently small, a (first order) Taylor series expansion can be used to approximate the inverse of the coupled impedance $\mathbf{Z}^{SI}_{c_1c_1}$ [16],

$$\left(\mathbf{Z}^{SI}_{c_1c_1}\right)^{-1} \approx \left(\mathbf{Z}^{S}_{c_1c_1}\right)^{-1} - \kappa\left(\mathbf{Z}^{S}_{c_1c_1}\right)^{-1}\mathbf{\Lambda}^{I}_{c_1c_1}\left(\mathbf{Z}^{S}_{c_1c_1}\right)^{-1}. \tag{26}$$

Substitution of Eqs. (25) and (26) into Eq. (12) then yields,

$$\bar{\mathbf{f}}^{SI_2}_{c_2} \approx \mathbf{Z}^{I_2}_{c_2c_1}\left(\left(\mathbf{Z}^{S}_{c_1c_1}\right)^{-1} - \kappa\left(\mathbf{Z}^{S}_{c_1c_1}\right)^{-1}\mathbf{\Lambda}^{I_2}_{c_1c_1}\left(\mathbf{Z}^{S}_{c_1c_1}\right)^{-1}\right)\left(\mathbf{Z}^{S}_{c_1c_1} + \kappa\,\mathbf{\Lambda}^{I_1}_{c_1c_1}\right)\left(\mathbf{Z}^{I_1}_{c_2c_1}\right)^{-1}\bar{\mathbf{f}}^{SI_1}_{c_2}. \tag{27}$$

Expanding the bracketed terms,

$$\bar{\mathbf{f}}^{SI_2}_{c_2} \approx \mathbf{Z}^{I_2}_{c_2c_1}\left(\mathbf{I} + \kappa\left(\mathbf{Z}^{S}_{c_1c_1}\right)^{-1}\mathbf{\Lambda}^{I_1}_{c_1c_1} - \kappa\left(\mathbf{Z}^{S}_{c_1c_1}\right)^{-1}\mathbf{\Lambda}^{I_2}_{c_1c_1} - \kappa^2\left(\mathbf{Z}^{S}_{c_1c_1}\right)^{-1}\mathbf{\Lambda}^{I_2}_{c_1c_1}\left(\mathbf{Z}^{S}_{c_1c_1}\right)^{-1}\mathbf{\Lambda}^{I_1}_{c_1c_1}\right)\left(\mathbf{Z}^{I_1}_{c_2c_1}\right)^{-1}\bar{\mathbf{f}}^{SI_1}_{c_2} \tag{28}$$

neglecting quadratic terms in κ (as we are considering a first order approximation),

$$\bar{\mathbf{f}}^{SI_2}_{c_2} \approx \mathbf{Z}^{I_2}_{c_2c_1}\left(\mathbf{I} + \kappa\left(\mathbf{Z}^{S}_{c_1c_1}\right)^{-1}\mathbf{\Lambda}^{I_1}_{c_1c_1} - \kappa\left(\mathbf{Z}^{S}_{c_1c_1}\right)^{-1}\mathbf{\Lambda}^{I_2}_{c_1c_1}\right)\left(\mathbf{Z}^{I_1}_{c_2c_1}\right)^{-1}\bar{\mathbf{f}}^{SI_1}_{c_2} \tag{29}$$

and substituting back $\kappa\,\mathbf{\Lambda}^{I}_{c_1c_1} = \mathbf{Z}^{I}_{c_1c_1}$, we arrive at,

$$\bar{\mathbf{f}}^{SI_2}_{c_2} \approx \mathbf{Z}^{I_2}_{c_2c_1}\left(\mathbf{I} + \left(\mathbf{Z}^{S}_{c_1c_1}\right)^{-1}\left[\mathbf{Z}^{I_1}_{c_1c_1} - \mathbf{Z}^{I_2}_{c_1c_1}\right]\right)\left(\mathbf{Z}^{I_1}_{c_2c_1}\right)^{-1}\bar{\mathbf{f}}^{SI_1}_{c_2} \tag{30}$$

or equivalently,

$$\bar{\mathbf{f}}^{SI_2}_{c_2} \approx \mathbf{Z}^{I_2}_{c_2c_1}\left(\mathbf{I} + \mathbf{Y}^{S}_{c_1c_1}\left[\mathbf{Z}^{I_1}_{c_1c_1} - \mathbf{Z}^{I_2}_{c_1c_1}\right]\right)\left(\mathbf{Z}^{I_1}_{c_2c_1}\right)^{-1}\bar{\mathbf{f}}^{SI_1}_{c_2}. \tag{31}$$

Eq. (31) constitutes a first order approximation of the modified blocked force $\bar{\mathbf{f}}^{SI_2}_{c_2}$, due to the component replacement $I_1 \rightarrow I_2$.

In the case that an identical mount is used ($I_1 = I_2$) the above yields, $\bar{\mathbf{f}}^{SI_2}_{c_2} = \bar{\mathbf{f}}^{SI_1}_{c_2}$, as expected. Although simplified, in its current form Eq. (31) still requires the free source mobility $\mathbf{Y}^{S}_{c_1c_1}$. However, it avoids the need for a double matrix inversion, as in Eq. (18). Matrix inversions are notoriously sensitive to experimental error and inconsistencies. As such, providing there is a sufficient impedance mismatch, Eq. (31) may provide a more reliable estimate than Eq. (18) in the presence of experimental uncertainty.

Note that in deriving Eq. 31 we considered the first order approximation of Eq. (12) (or equivalently Eq. (17)). Had we applied the approximation to Eq. (19) we would have arrived at the intermediate form,

$$\bar{\mathbf{f}}^{SI_2}_{c_2} \approx \mathbf{Z}^{I_2}_{c_2c_1}\left[\mathbf{I} + \left(\mathbf{Z}^{SI_1}_{c_1c_1}\right)^{-1}\left(\mathbf{Z}^{I_1}_{c_1c_1} - \mathbf{Z}^{I_2}_{c_1c_1}\right)\right]\left(\mathbf{Z}^{I_1}_{c_2c_1}\right)^{-1}\bar{\mathbf{f}}^{SI_1}_{c_2} \tag{32}$$

where the coupled *SI* impedance $\mathbf{Z}^{SI_1}_{c_1c_1}$ replaces the free source mobility. Recall that this impedance term is available in-situ, as per Eq. (20). Hence, Eq. (32) constitutes an in-situ first order approximation. This form may prove useful if the free mobility is not available. Note that if we were to apply a first order approximation to the inverse of $\mathbf{Z}^{SI_1}_{c_1c_1}$ we would arrive identically at Eq. (31). Whilst Eq. (32) no longer requires the free source mobility, it does still require response measurements above and below the coupling element. Often, due to limited channel count, available sensors, or restricted access, it is not possible to obtain the required source side response measurements. Hence, we are interested in further simplifying the above component replacement expressions.

Note that the free source mobility in Eq. (31) is multiplied by a small quantity; the coupling element impedance difference $\mathbf{Z}^{I_1}_{c_1c_1} - \mathbf{Z}^{I_2}_{c_1c_1}$. It is argued that, provided the elements are not too dissimilar, a reasonable approximation can be obtained from the zeroth order term alone,

$$\bar{\mathbf{f}}^{SI_2}_{c_2} \approx \mathbf{Z}^{I_2}_{c_2c_1}\left(\mathbf{Z}^{I_1}_{c_2c_1}\right)^{-1}\bar{\mathbf{f}}^{SI_1}_{c_2}. \tag{33}$$

Eq. (33) constitutes a zeroth order approximation to the modified blocked force $\bar{\mathbf{f}}^{SI_2}_{c_2}$, due to the component replacement $I_1 \rightarrow I_2$. Importantly, Eq. (33) requires only the transfer impedance of the two coupling elements, and thus avoids the need to perform any additional measurements over and above those required by a standard in-situ TPA.

In general, the matrix product $\mathbf{Z}^{I_2}_{c_2c_1}\left(\mathbf{Z}^{I_1}_{c_2c_1}\right)^{-1}$ may be fully populated. In the simplified case where no cross-coupling exists between the primary and secondary interface DoFs, we have that,

$$\mathbf{Z}^{I_2}_{c_2c_1}\left(\mathbf{Z}^{I_1}_{c_2c_1}\right)^{-1} \rightarrow \begin{bmatrix} \alpha_1 & 0 & 0 \\ 0 & \ddots & 0 \\ 0 & 0 & \alpha_N \end{bmatrix} \tag{34}$$

Table 1
Summary of Component Replacement TPA equations for an upstream modification of the blocked force and forward transfer function.

Approx.	Modified blocked force: $\tilde{\mathbf{f}}_{c_2}^{SI_2} = \mathbf{T}_{\tilde{\mathbf{f}}}^{(I_2 \leftarrow I_1)} \tilde{\mathbf{f}}_{c_2}^{SI_1}$	Modified transfer function: $\mathbf{Y}_{rc_2}^{C_2} = \mathbf{Y}_{rc_2}^{C_1} \mathbf{T}_{\mathbf{Y}}^{C_2 (I_2 \leftarrow I_1)}$
Exact	$\mathbf{T}_{\tilde{\mathbf{f}}} = \mathbf{Z}_{c_2c_1}^{I_2} \left(\left(\mathbf{Y}_{c_1c_1}^{S} \right)^{-1} + \mathbf{Z}_{c_1c_1}^{I_2} \right)^{-1} \left(\left(\mathbf{Y}_{c_1c_1}^{S} \right)^{-1} + \mathbf{Z}_{c_1c_1}^{I_1} \right) \left(\mathbf{Z}_{c_2c_1}^{I_1} \right)^{-1}$ $\mathbf{T}_{\tilde{\mathbf{f}}} = \mathbf{Z}_{c_2c_1}^{I_2} \left(\mathbf{Z}_{c_1c_1}^{SI_1} + \left[\mathbf{Z}_{c_1c_1}^{I_2} - \mathbf{Z}_{c_1c_1}^{I_1} \right] \right)^{-1} \mathbf{Z}_{c_1c_1}^{SI_1} \left(\mathbf{Z}_{c_2c_1}^{I_1} \right)^{-1}$	$\mathbf{T}_{\mathbf{Y}}^{C_2} = \left(\mathbf{Y}_{c_2c_2}^{C_1} \right)^{-1} \left[\left(\mathbf{Y}_{c_2c_2}^{C_1} \right)^{-1} + \left(\mathbf{Z}_{c_2c_2}^{SI_2} - \mathbf{Z}_{c_2c_2}^{SI_1} \right) \right]^{-1}$
First order	$\mathbf{T}_{\tilde{\mathbf{f}}} \approx \mathbf{Z}_{c_2c_1}^{I_2} \left[\mathbf{I} + \mathbf{Y}_{c_1c_1}^{S} \left(\mathbf{Z}_{c_1c_1}^{I_1} - \mathbf{Z}_{c_1c_1}^{I_2} \right) \right] \left(\mathbf{Z}_{c_2c_1}^{I_1} \right)^{-1}$ $\mathbf{T}_{\tilde{\mathbf{f}}} \approx \mathbf{Z}_{c_2c_1}^{I_2} \left[\mathbf{I} + \left(\mathbf{Z}_{c_1c_1}^{SI_1} \right)^{-1} \left(\mathbf{Z}_{c_1c_1}^{I_1} - \mathbf{Z}_{c_1c_1}^{I_2} \right) \right] \left(\mathbf{Z}_{c_2c_1}^{I_1} \right)^{-1}$	$\mathbf{T}_{\mathbf{Y}}^{C_2} \approx \left[\mathbf{I} - \left(\mathbf{Z}_{c_2c_2}^{I_2} - \mathbf{Z}_{c_2c_2}^{I_1} \right) \mathbf{Y}_{c_2c_2}^{C_1} \right]$
Zeroth order	$\mathbf{T}_{\tilde{\mathbf{f}}} \approx \mathbf{Z}_{c_2c_1}^{I_2} \left(\mathbf{Z}_{c_2c_1}^{I_1} \right)^{-1}$	$\mathbf{T}_{\mathbf{Y}}^{C_2} \approx \mathbf{I}$

where $\alpha_N = Z_{c_{2N}c_{1N}}^{I_2} / Z_{c_{2N}c_{1N}}^{I_1}$ is the ratio of the Nth element's initial to modified transfer impedance. In a design optimisation context, this ratio could be used to determine the necessary modification required to achieve a specified target response level.

In summary, Eqs. (12), (31), and (33), provide, respectively, an exact, first order, and zeroth order approximation to the modified blocked force $\tilde{\mathbf{f}}_{c_2}^{SI_2}$ due to the component replacement $I_1 \rightarrow I_2$. These equations are summarized in Table 1.

3.2. Modified forward transfer function

Eqs. (12), (31), and (33), enable the modification of the secondary interface blocked force $\tilde{\mathbf{f}}_{c_2}^{SI}$ given the component replacement $I_1 \rightarrow I_2$. To make a TPA response prediction in this modified assembly, the (modified) blocked force must be accompanied by an appropriately modified forward transfer function $\mathbf{Y}_{rc_2}^{C_2}$. In this section we will derive a modification of the initial forward transfer function $\mathbf{Y}_{rc_2}^{C_1}$ to accompany the modified blocked force $\tilde{\mathbf{f}}_{c_2}^{SI_2}$.

We begin by recalling the invariant properties of the transmissibility [17]. It can been shown that the velocity transmissibility between the interface DoFs c_2 and the remote target DoFs r, due to an applied force at c_2, $\mathbf{T}_{rc_2}^{C_2}$, is independent of the forcing applied. Consequently, the same transmissibility would be obtained whether or not the SI assembly is attached to the receiver R. As such, we have that,

$$\mathbf{Y}_{rc_2}^{C} \left(\mathbf{Y}_{c_2c_2}^{C} \right)^{-1} = \mathbf{Y}_{rc_2}^{R} \left(\mathbf{Y}_{c_2c_2}^{R} \right)^{-1} = \mathbf{T}_{rc_2}^{c_2}. \tag{35}$$

Based on this invariance, a second equation can be established for a new assembly (C_2) whose coupling element has been replaced,

$$\mathbf{Y}_{rc_2}^{C_2} \left(\mathbf{Y}_{c_2c_2}^{C_2} \right)^{-1} = \mathbf{Y}_{rc_2}^{R} \left(\mathbf{Y}_{c_2c_2}^{R} \right)^{-1}. \tag{36}$$

The left hand sides of Eqs. (35) and (36) can now be equated. Post-multiplication by $\mathbf{Y}_{c_2c_2}^{C_2}$ then yields,

$$\mathbf{Y}_{rc_2}^{C_2} = \mathbf{Y}_{rc_2}^{C_1} \left(\mathbf{Y}_{c_2c_2}^{C_1} \right)^{-1} \mathbf{Y}_{c_2c_2}^{C_2} \tag{37}$$

where the superscript C_1 is used to denote the initial assembly.

Eq. (37) provides an exact modification of the forward transfer function $\mathbf{Y}_{rc_2}^{C_1}$, due to the component replacement $I_1 \rightarrow I_2$. This form, however, requires the modified assembly's point mobility matrix $\mathbf{Y}_{c_2c_2}^{C_2}$, which is unavailable. To simplify Eq. (37) we begin by substituting the modified mobility $\mathbf{Y}_{c_2c_2}^{C_2}$ for its impedance form,

$$\mathbf{Y}_{rc_2}^{C_2} = \mathbf{Y}_{rc_2}^{C_1} \left(\mathbf{Y}_{c_2c_2}^{C_1} \right)^{-1} \left(\mathbf{Z}_{c_2c_2}^{R} + \mathbf{Z}_{c_2c_2}^{SI_2} \right)^{-1} \tag{38}$$

where $\mathbf{Z}_{c_2c_2}^{SI_2}$ represents the point impedance of the modified source-coupling assembly. By adding and subtracting the initial source-coupling impedance $\mathbf{Z}_{c_2c_2}^{SI_1}$,

$$\mathbf{Y}_{rc_2}^{C_2} = \mathbf{Y}_{rc_2}^{C_1} \left(\mathbf{Y}_{c_2c_2}^{C_1} \right)^{-1} \left(\mathbf{Z}_{c_2c_2}^{R} + \mathbf{Z}_{c_2c_2}^{SI_2} + \mathbf{Z}_{c_2c_2}^{SI_1} - \mathbf{Z}_{c_2c_2}^{SI_1} \right)^{-1} \tag{39}$$

and rearranging terms, we arrive at,

$$\mathbf{Y}_{rc_2}^{C_2} = \mathbf{Y}_{rc_2}^{C_1} \left(\mathbf{Y}_{c_2c_2}^{C_1} \right)^{-1} \left(\mathbf{Z}_{c_2c_2}^{C_1} + \left(\mathbf{Z}_{c_2c_2}^{SI_2} - \mathbf{Z}_{c_2c_2}^{SI_1} \right) \right)^{-1} \tag{40}$$

where $\mathbf{Z}_{c_2c_2}^{C_1}$ is the coupled impedance of the initial assembly. Eq. (40) remains exact, as no approximations have been introduced.

As with the modified blocked force, we consider the special case of a resilient coupling element, and the presence of an impedance mismatch, now between the receiver and source-coupling assembly. By approximating the rightmost matrix inverse of Eq. (40) as a first order Taylor expansion,

$$\mathbf{Y}_{rc_2}^{C_2} \approx \mathbf{Y}_{rc_2}^{C_1} \left(\mathbf{Y}_{c_2c_2}^{C_1} \right)^{-1} \left[\mathbf{Y}_{c_2c_2}^{C_1} - \mathbf{Y}_{c_2c_2}^{C_1} \left(\mathbf{Z}_{c_2c_2}^{SI_2} - \mathbf{Z}_{c_2c_2}^{SI_1} \right) \mathbf{Y}_{c_2c_2}^{C_1} \right] \tag{41}$$

we arrive at the simplified equation,

$$\mathbf{Y}^{C_2}_{rc_2} \approx \mathbf{Y}^{C_1}_{rc_2}\left[\mathbf{I} - \left(\mathbf{Z}^{SI_2}_{c_2c_2} - \mathbf{Z}^{SI_1}_{c_2c_2}\right)\mathbf{Y}^{C_1}_{c_2c_2}\right]. \tag{42}$$

Eq. (42) constitutes a first order approximation of the modified forward transfer function $\mathbf{Y}^{C_2}_{rc_2}$, due to the component replacement $I_1 \rightarrow I_2$.

It is important to note that the impedance terms $\mathbf{Z}^{SI_2}_{c_2c_2}$ and $\mathbf{Z}^{SI_2}_{c_2c_2}$ are properties of the source-coupling assembly *SI*, and include dynamic contributions from both the source and the coupling element; these are not directly available from experiment. We are interested in simplifying the impedance difference $\mathbf{Z}^{SI_2}_{c_2c_2} - \mathbf{Z}^{SI_1}_{c_2c_2}$ such that it can be expressed in terms of available quantities. Under the present assumptions (i.e. an impedance mismatch) the source will have a high impedance compared to the coupling element. As such, the coupling element will be *approximately* blocked at the primary interface, and $\mathbf{Z}^{SI}_{c_2c_2} \approx \mathbf{Z}^{I}_{c_2c_2}$. This same conclusion can be arrived at by a first order approximation as follows.

Consider the source-coupling assembly *SI*, whose secondary interface is excited by an external force,

$$\begin{pmatrix}\mathbf{v}_{c_1}\\ \mathbf{v}_{c_2}\end{pmatrix} = \begin{pmatrix}\mathbf{Y}^{SI}_{c_1c_1} & \mathbf{Y}^{SI}_{c_1c_2}\\ \mathbf{Y}^{SI}_{c_2c_1} & \mathbf{Y}^{SI}_{c_2c_2}\end{pmatrix}\begin{pmatrix}\mathbf{0}\\ \mathbf{f}_{c_2}\end{pmatrix}. \tag{43}$$

Equivalently in impedance form,

$$\begin{pmatrix}\mathbf{0}\\ \mathbf{f}_{c_2}\end{pmatrix} = \begin{pmatrix}\mathbf{Z}^{SI}_{c_1c_1} & \mathbf{Z}^{I}_{c_1c_2}\\ \mathbf{Z}^{I}_{c_2c_1} & \mathbf{Z}^{I}_{c_2c_2}\end{pmatrix}\begin{pmatrix}\mathbf{v}_{c_1}\\ \mathbf{v}_{c_2}\end{pmatrix} \tag{44}$$

where it is noted that $\left(\mathbf{Z}^{I}_{c_2c_2}\right)^{-1} \neq \mathbf{Y}^{SI}_{c_2c_2}$. The top row of Eq. (44) can be rearranged for the primary interface velocity,

$$\mathbf{0} = \mathbf{Z}^{SI}_{c_1c_1}\mathbf{v}_{c_1} + \mathbf{Z}^{I}_{c_1c_2}\mathbf{v}_{c_2} \rightarrow \mathbf{v}_{c_1} = -\left(\mathbf{Z}^{SI}_{c_1c_1}\right)^{-1}\mathbf{Z}^{I}_{c_1c_2}\mathbf{v}_{c_2} \tag{45}$$

and substituted it into the bottom row of Eq. (44) to give,

$$\mathbf{f}_{c_2} = \left(-\mathbf{Z}^{I}_{c_2c_1}\left(\mathbf{Z}^{SI}_{c_1c_1}\right)^{-1}\mathbf{Z}^{I}_{c_1c_2} + \mathbf{Z}^{I}_{c_2c_2}\right)\mathbf{v}_{c_2} = \left(-\mathbf{Z}^{I}_{c_2c_1}\left(\left(\mathbf{Y}^{S}_{c_1c_1}\right)^{-1} + \mathbf{Z}^{I}_{c_1c_1}\right)^{-1}\mathbf{Z}^{I}_{c_1c_2} + \mathbf{Z}^{I}_{c_2c_2}\right)\mathbf{v}_{c_2} = \tilde{\mathbf{Z}}^{SI}_{c_2c_2}\mathbf{v}_{c_2} \tag{46}$$

where $\tilde{\mathbf{Z}}^{SI}_{c_2c_2}$ represents a reduced impedance matrix which takes into account the dynamics of the source. Note that Eq. (46) represents the same dynamic system as Eqs. (43) and (44). Consequently, $\left(\tilde{\mathbf{Z}}^{SI}_{c_2c_2}\right)^{-1} = \mathbf{Y}^{SI}_{c_2c_2}$, and the *SI* impedance terms in Eqs. (40) and (42) may be expressed in the form of Eq. (46).

In the presence of an impedance mismatch, the reduced impedance matrix may be rewritten in the form,

$$\tilde{\mathbf{Z}}^{SI}_{c_2c_2} = \left(-\kappa^2\mathbf{\Lambda}^{I}_{c_2c_1}\left(\mathbf{Z}^{S}_{c_1c_1} + \kappa\mathbf{\Lambda}^{I}_{c_1c_1}\right)^{-1}\mathbf{\Lambda}^{I}_{c_1c_2} + \kappa\mathbf{\Lambda}^{I}_{c_2c_2}\right) \tag{47}$$

which, after applying a first order Taylor expansion to the matrix inverse, yields,

$$\tilde{\mathbf{Z}}^{SI}_{c_2c_2} = \left(-\kappa^2\mathbf{\Lambda}^{I}_{c_2c_1}\left[\left(\mathbf{Z}^{S}_{c_1c_1}\right)^{-1} - \kappa\left(\mathbf{Z}^{S}_{c_1c_1}\right)^{-1}\mathbf{\Lambda}^{I}_{c_1c_1}\left(\mathbf{Z}^{S}_{c_1c_1}\right)^{-1}\right]\mathbf{\Lambda}^{I}_{c_1c_2} + \kappa\mathbf{\Lambda}^{I}_{c_2c_2}\right). \tag{48}$$

If we retain only first order terms in κ, the above reduces to,

$$\tilde{\mathbf{Z}}^{SI}_{c_2c_2} \approx \mathbf{Z}^{I}_{c_2c_2}. \tag{49}$$

Given that Eq. (42) is already based on a first order approximation, Eq. (49) may be incorporated as so,

$$\mathbf{Y}^{C_2}_{rc_2} \approx \mathbf{Y}^{C_1}_{rc_2}\left[\mathbf{I} - \left(\mathbf{Z}^{I_2}_{c_2c_2} - \mathbf{Z}^{I_1}_{c_2c_2}\right)\mathbf{Y}^{C_1}_{c_2c_2}\right]. \tag{50}$$

Eq. (50) constitutes a first order approximation of the modified forward transfer function $\mathbf{Y}^{C_2}_{rc_2}$, due to the component replacement $I_1 \rightarrow I_2$.

Finally, from Eqs. (50) (or (42)) a zeroth order approximation can be identified as simply,

$$\mathbf{Y}^{C_2}_{rc_2} \approx \mathbf{Y}^{C_1}_{rc_2} \tag{51}$$

i.e. the component replacement has no effect on the forward transfer function.

In summary, Eqs. (37), (50), and (51), provide, respectively, an exact, first order, and zeroth order approximation to the modified forward transfer function $\mathbf{Y}^{C_2}_{rc_2}$ due to the component replacement $I_1 \rightarrow I_2$. These equations are summarized in Table 1.

3.3. Summary of Component Replacement TPA equations

The purpose of this paper has been to derive a set of equations that relate the blocked force and forward transfer function of an initial assembly, to those of an *upstream modified* assembly, where a sub-component of the source has been modified or replaced. In contrast to conventional component-based TPA, which aims to build an assembly from the measurement of individual components, the proposed CR-TPA begins with an initial (coupled) assembly, and seeks to replace or modify

a component. Hence, CR-TPA may be viewed as an extension of in-situ TPA, enabling the upstream (also downstream, see Appendix A) structural modification of an assembly for design optimisation.

The CR-TPA equations derived above can be expressed generally in the form,

$$\tilde{\mathbf{f}}_{c_2}^{SI_2} = \mathbf{T}_{\tilde{\mathbf{f}}}^{(I_2 \leftarrow I_1)} \tilde{\mathbf{f}}_{c_2}^{SI_1} \tag{52}$$

and

$$\mathbf{Y}_{rc_2}^{C_2} = \mathbf{Y}_{rc_2}^{C_1} \mathbf{T}_{\mathbf{Y}}^{c_2\,(I_2 \leftarrow I_1)} \tag{53}$$

where Eq. (52) constitutes a modification of the blocked force, and Eq. (53) the forward transfer function. The corresponding 'transmodification' matrices $\mathbf{T}_{\tilde{\mathbf{f}}}^{(I_2 \leftarrow I_1)}$ and $\mathbf{T}_{\mathbf{Y}}^{c_2\,(I_2 \leftarrow I_1)}$ characterise the component replacement $I_1 \rightarrow I_2$.[12] Their form depends on whether an exact, first order or zeroth order modification is considered. The corresponding equations are summarised in Table 1.

The exact transmodification matrices were derived irrespective of the nature of the coupling element I. Hence, they are valid in the presence of an arbitrary coupling element. This benefit comes at the cost of additional complexity and experimental effort. Providing the point and transfer impedance of the initial and replacement coupling elements are already known, $\mathbf{T}_{\tilde{\mathbf{f}}}$ requires either the free source mobility $\mathbf{Y}_{c_1c_1}^{S}$, or the source-coupling impedance $\mathbf{Z}_{c_1c_1}^{SI_1}$. The former requires dismantling the assembly to freely suspend the source, whilst the latter requires instrumentation of both the primary and secondary interfaces (see Eq. (20)). Similarly, $\mathbf{T}_{\mathbf{Y}}^{c_2}$ requires the initial and replacement source-coupling impedance $\mathbf{Z}_{c_2c_2}^{SI}$. Whilst this term can be calculated as per Eq. (46), the free source mobility is still required. Furthermore, in the exact case both $\mathbf{T}_{\tilde{\mathbf{f}}}$ and $\mathbf{T}_{\mathbf{Y}}^{c_2}$ require a double matrix inversion. Matrix inversions are known to amplify the effect of noise, and so the exact formulation may be more sensitive to experimental error.

In the presence of a resilient coupling (which would typically be the case for vibrating machinery) an impedance mismatch can be assumed at the primary and secondary interfaces and, by use of a Taylor series expansion, first and zeroth order approximations can be derived. The first order transmodification matrices have the advantage that they avoid the need for a double matrix inversion. Hence, they are likely less sensitive to experimental error. Whilst $\mathbf{T}_{\tilde{\mathbf{f}}}$ still requires the free source mobility (or source-coupling impedance), $\mathbf{T}_{\mathbf{Y}}^{c_2}$ requires only the initial assembly mobility, and the initial and replacement coupling element impedance; the source-coupling impedance required by the exact modification is reduced to the coupling impedance alone.

Finally, the zeroth order transmodification matrices provide what is perhaps the most useful form of CR-TPA. $\mathbf{T}_{\tilde{\mathbf{f}}}$ reduces simply to a product of the modified and (inverse) initial coupling impedance; the free source mobility is no longer required. $\mathbf{T}_{\mathbf{Y}}^{c_2}$ takes the even simpler form of an identity matrix. Although a lower order approximation, the zeroth order case is likely the most practical given its simple form and the minimal experimental effort required (all that is needed is the transfer impedance of the initial and replacement coupling elements). It is shown later in Section 4.2.3, as part of a numerical example, that the zeroth order errors are not significantly greater than that of the first order approximation, and that for a reasonable impedance mismatch errors of less than 5dB can be expected.

4. Numerical case study

In this section two numerical examples are presented. They will demonstrate the application of CR-TPA to the exact and approximate prediction of modified blocked forces and forward transfer functions, due to an upstream component replacement. An experimental illustration of CR-TPA can be found in [18], where the method is used to replace the resilient mounts of an automotive gearbox, and predict the resulting cabin sound pressure level.

4.1. Coupled beam assembly

This initial example is shown diagrammatically in Fig. 2; two free-free beams (source and receiver) are coupled via a third (resilient) beam element. As above, we identify the primary and secondary interfaces as c_1 and c_2, respectively. We are interested in predicting the blocked force at, and the forward transfer function from, the secondary interface c_2 based on the modification of some initial assembly. This modification will be the replacement of the resilient coupling by another of different geometry and material properties. Results will be compared against those obtained directly from the modified assembly. The geometry and material properties of each beam element are given in Table 2.

The initial blocked force $\tilde{\mathbf{f}}_{c_2}^{SI_1} \in \mathbb{C}^2$ is obtained using the inverse relation of Eq. (1) based on the mobility of the coupled *SIR* assembly. The initial forward transfer function $\mathbf{Y}_{rc_2}^{C_1} \in \mathbb{C}^{1\times 2}$ is obtained from the same assembly. These are shown in grey in Figs. 3 and 4, respectively. Two plots are shown in each figure, corresponding to the blocked force (a) and the blocked moment (b) in Fig. 3, and their associated transfer functions in Fig. 4.

[1] Whilst $\mathbf{T}_{\tilde{\mathbf{f}}}^{(I_2 \leftarrow I_1)}$ and $\mathbf{T}_{\mathbf{Y}}^{c_2\,(I_2 \leftarrow I_1)}$ were derived based on the principles of transmissibility, strictly speaking they are not transmissibilities in the traditional sense. Transmissibilities relate like-quantities between DoFs on the same assembly. In contrast, $\mathbf{T}_{\tilde{\mathbf{f}}}^{(I_2 \leftarrow I_1)}$ and $\mathbf{T}_{\mathbf{Y}}^{c_2\,(I_2 \leftarrow I_1)}$ relate the blocked force and forward transfer function between the same DoFs of two different assemblies. Hence, the term 'transmodification' is deemed more appropriate.

[2] The superscript c_2 of $\mathbf{T}_{\mathbf{Y}}^{c_2\,(I_2 \leftarrow I_1)}$ is used to denote the secondary interface from which the modification is considered. In Appendix A we consider a component replacement from the perspective of the primary interface c_1 and derive the transmodification matrix $\mathbf{T}_{\mathbf{Y}}^{c_1\,(I_2 \leftarrow I_1)}$.

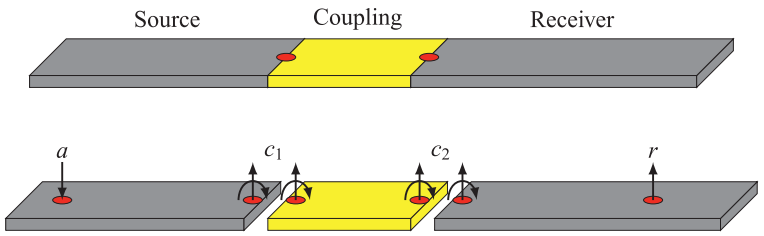

Fig. 2. Diagram of numerical simulation; two steel beams coupled via a third resilient beam.

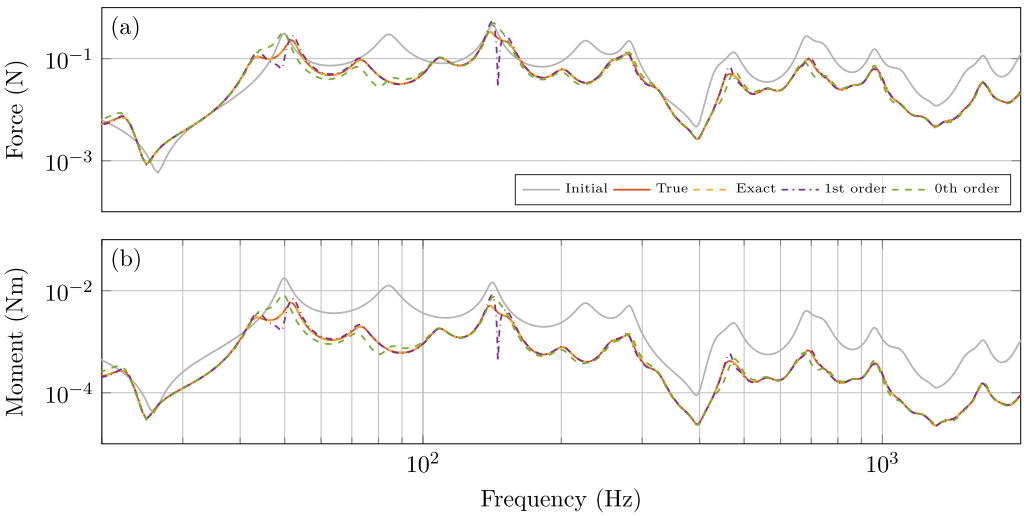

Fig. 3. Modified blocked force at the interface c_2 obtained using the Component Replacement TPA approach and its approximations; (a) - blocked force, (b) - blocked moment. Grey plot corresponds to the blocked force obtained for the initial assembly. Remaining plots correspond to the new assembly with a component replacement.

Table 2
Beam element properties - l length, E Young's modulus, ρ density, and η loss factor. All beam elements were given a thickness h of 0.01 m and a width w of 0.1 m.

Element	l (m)	E (GPa)	ρ (kg/m^3)	η
Source	1	200	7800	0.05
Receiver	0.5	200	7800	0.1
Coupling (init.)	0.2	2	2000	0.1
Coupling (mod.)	0.3	0.2	4000	0.1

The same procedure is followed for the modified assembly, and the true blocked force and transfer function are obtained. These are shown in orange in Figs. 3 and 4, respectively. The purpose of CR-TPA is to predict these modified assembly properties based on those of the initial assembly.

Comparison of the initial and (true) modified blocked force in Fig. 3 demonstrates the large effect the modification of a coupling element can have on the blocked force at the secondary interface. Fig. 4 suggests this modification has a lesser effect on the forward transfer function. This is to be expected given the resilient nature of the coupling.

Also shown in Fig. 3 are the exact (yellow), first order (purple), and zeroth order (green) blocked force predictions obtained as per Table 1. As expected, the exact modification is in agreement with the true blocked force. The first order approximation can be seen to provide a good estimate of the blocked force across most of the frequency range, although there are some notable discrepancies (see for example $\approx$150 Hz). The zeroth order approximation also provides a reasonable estimate given its simplicity.

Shown in Fig. 4 are the exact (yellow), and first order (purple) transfer function predictions obtained as per Table 1 (the zeroth order approximation corresponds to the unmodified transfer function). Again, the exact modification is in agreement with the true transfer function. The first order approximation can be seen to provide a noticeable improvement over the unmodified transfer function.

These results demonstrate the application of CR-TPA, albeit on a simple assembly. In the following sub-section a more complex numerical assembly will be considered.

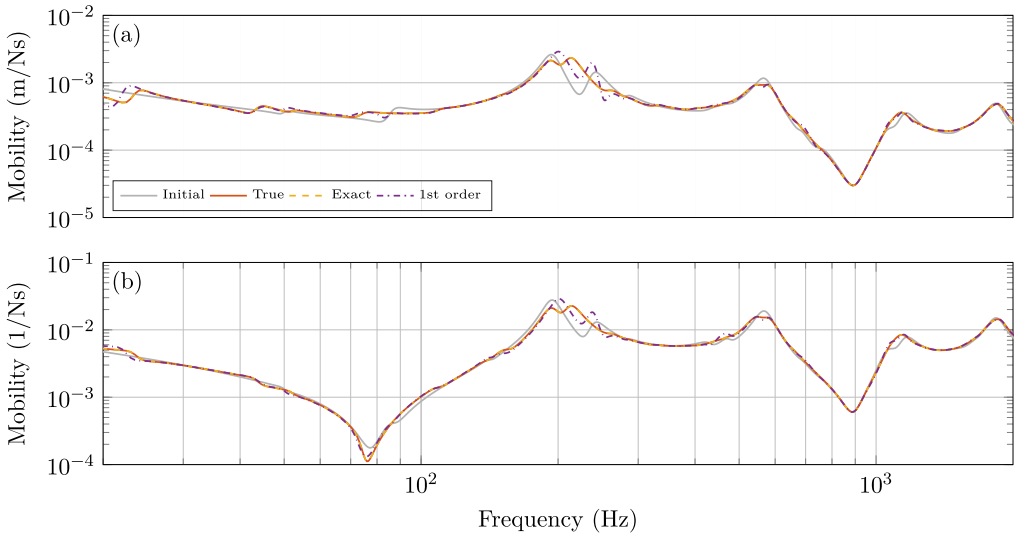

Fig. 4. Modified forward transfer function between the interface and reference DoFs c_2 and r obtained using the Component Replacement TPA approach and its approximations; (a) - force-velocity mobility, (b) - moment-velocity mobility. Grey plot corresponds to the transfer function obtained for the initial assembly. Remaining plots correspond to the new assembly with a component replacement.

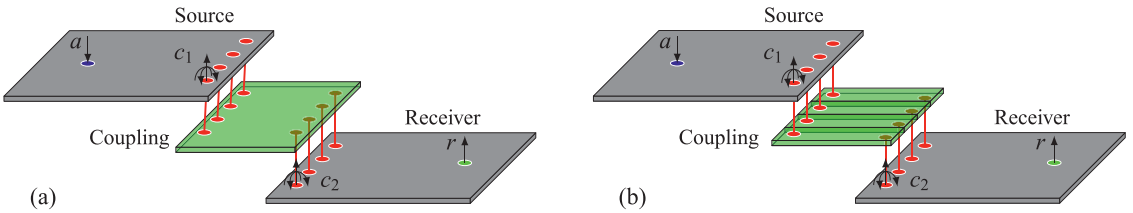

Fig. 5. Schematic of the numerical examples considered; (a) - fully connected coupling element, (b) - discrete coupling elements.

Table 3
Plate element properties - l length, w width, h thickness, E Young's modulus, ρ density, and η loss factor.

Element	$l \times w \times h$ (m)	E (GPa)	ρ (kg/m^3)	η
Source	$0.6 \times 0.5 \times 0.01$	200	7800	0.05
Receiver	$0.6 \times 0.5 \times 0.01$	200	7800	0.05
Coupling (connected, init.)	$0.35 \times 0.5 \times 0.005$	0.2	4000	0.05
Coupling (connected, mod.)	$0.45 \times 0.5 \times 0.005$	2	2000	0.1
Coupling (discrete, init.)	$0.35 \times 0.1 \times 0.005$	0.2	4000	0.05
Coupling (discrete, mod.)	$0.45 \times 0.1 \times 0.005$	2	2000	0.1

4.2. Complex plate assembly

The study considered here is shown diagrammatically in Fig. 5; two free-free plates (source and receiver) are coupled via a third plate-like element. This assembly is more complex than the previous, with a closer resemblance to practical applications of the method. As above, we identify the primary and secondary interfaces as c_1 and c_2, respectively. In the present case study these interfaces include several points of contact, each having DoFs in the out-of-plane z direction, and rotation about the x/y axes (see Fig. 5). We are interested in predicting the blocked force at, and the forward transfer function from, the secondary interface c_2 based on the modification of some initial assembly. This modification will be the replacement of the coupling element by another of different geometry and material properties. Note that again a resilient coupling has been considered to demonstrate the application of the first and zeroth order approximations.

Two particular cases will be explored; a fully connected coupling element where all interface DoFs are coupled via a single component (see Fig. 5a), and a series of discrete coupling elements where each interface contact is coupled to just one other (see Fig. 5b). The CR-TPA results will be compared against those obtained directly from the modified assemblies. The geometry and material properties of each plate element are given in Table 3.

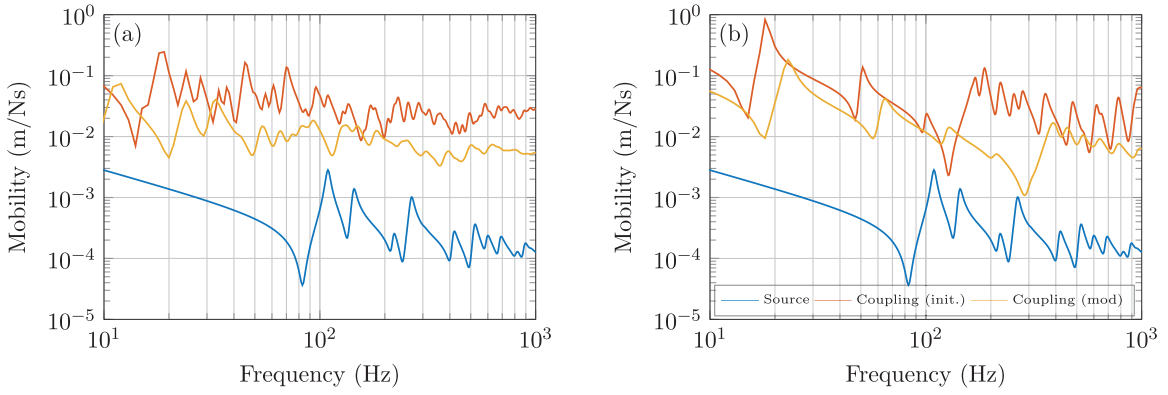

Fig. 6. Example point mobilities for the uncoupled source and the fully connected (a) and discrete (b) coupling elements shown in Fig. 5a and 5b, respectively. Initial couplings are shown in orange, and modified in yellow. (For interpretation of the references to color in this figure legend, the reader is referred to the web version of this article.)

The fundamental difference between the two assemblies considered here is the structure of their coupling element's impedance matrix $\mathbf{Z_I} \in \mathbb{C}^{24\times24}$. The fully connected coupling is described by the full impedance matrix,

$$\mathbf{Z}^I = \begin{bmatrix} \mathbf{Z}_{11,11} & \mathbf{Z}_{11,12} & \mathbf{Z}_{11,13} & \mathbf{Z}_{11,14} & \mathbf{Z}_{11,21} & \mathbf{Z}_{11,22} & \mathbf{Z}_{11,23} & \mathbf{Z}_{11,24} \\ \mathbf{Z}_{12,11} & \mathbf{Z}_{12,12} & \mathbf{Z}_{12,13} & \mathbf{Z}_{12,14} & \mathbf{Z}_{12,21} & \mathbf{Z}_{12,22} & \mathbf{Z}_{12,23} & \mathbf{Z}_{12,24} \\ \mathbf{Z}_{13,11} & \mathbf{Z}_{13,12} & \mathbf{Z}_{13,13} & \mathbf{Z}_{13,14} & \mathbf{Z}_{13,21} & \mathbf{Z}_{13,22} & \mathbf{Z}_{13,23} & \mathbf{Z}_{13,24} \\ \mathbf{Z}_{14,11} & \mathbf{Z}_{14,12} & \mathbf{Z}_{14,13} & \mathbf{Z}_{14,14} & \mathbf{Z}_{14,21} & \mathbf{Z}_{14,22} & \mathbf{Z}_{14,23} & \mathbf{Z}_{14,24} \\ \mathbf{Z}_{21,11} & \mathbf{Z}_{21,12} & \mathbf{Z}_{21,13} & \mathbf{Z}_{21,14} & \mathbf{Z}_{21,21} & \mathbf{Z}_{21,22} & \mathbf{Z}_{21,23} & \mathbf{Z}_{21,24} \\ \mathbf{Z}_{22,11} & \mathbf{Z}_{22,12} & \mathbf{Z}_{22,13} & \mathbf{Z}_{22,14} & \mathbf{Z}_{22,21} & \mathbf{Z}_{22,22} & \mathbf{Z}_{22,23} & \mathbf{Z}_{22,24} \\ \mathbf{Z}_{23,11} & \mathbf{Z}_{23,12} & \mathbf{Z}_{23,13} & \mathbf{Z}_{23,14} & \mathbf{Z}_{23,21} & \mathbf{Z}_{23,22} & \mathbf{Z}_{23,23} & \mathbf{Z}_{23,24} \\ \mathbf{Z}_{24,11} & \mathbf{Z}_{24,12} & \mathbf{Z}_{24,13} & \mathbf{Z}_{24,14} & \mathbf{Z}_{24,21} & \mathbf{Z}_{24,22} & \mathbf{Z}_{24,23} & \mathbf{Z}_{24,24} \end{bmatrix}. \tag{54}$$

whilst the discrete coupling element impedance is given by,

$$\mathbf{Z}^I = \begin{bmatrix} \mathbf{Z}_{11,11} & \mathbf{0} & \mathbf{0} & \mathbf{0} & \mathbf{Z}_{11,21} & \mathbf{0} & \mathbf{0} & \mathbf{0} \\ \mathbf{0} & \mathbf{Z}_{12,12} & \mathbf{0} & \mathbf{0} & \mathbf{0} & \mathbf{Z}_{12,22} & \mathbf{0} & \mathbf{0} \\ \mathbf{0} & \mathbf{0} & \mathbf{Z}_{13,13} & \mathbf{0} & \mathbf{0} & \mathbf{0} & \mathbf{Z}_{13,23} & \mathbf{0} \\ \mathbf{0} & \mathbf{0} & \mathbf{0} & \mathbf{Z}_{14,14} & \mathbf{0} & \mathbf{0} & \mathbf{0} & \mathbf{Z}_{14,24} \\ \mathbf{Z}_{21,11} & \mathbf{0} & \mathbf{0} & \mathbf{0} & \mathbf{Z}_{21,21} & \mathbf{0} & \mathbf{0} & \mathbf{0} \\ \mathbf{0} & \mathbf{Z}_{22,12} & \mathbf{0} & \mathbf{0} & \mathbf{0} & \mathbf{Z}_{22,22} & \mathbf{0} & \mathbf{0} \\ \mathbf{0} & \mathbf{0} & \mathbf{Z}_{23,13} & \mathbf{0} & \mathbf{0} & \mathbf{0} & \mathbf{Z}_{23,23} & \mathbf{0} \\ \mathbf{0} & \mathbf{0} & \mathbf{0} & \mathbf{Z}_{24,14} & \mathbf{0} & \mathbf{0} & \mathbf{0} & \mathbf{Z}_{24,24} \end{bmatrix} \tag{55}$$

where subscript ij,kl denotes the impedance between the jth contact on the ith interface, and the lth contact on the kth interface. Note that each impedance sub-matrix contains translational and rotational components, $\mathbf{Z}_{ij,kl} \in \mathbb{C}^{3\times3}$.

Topologically, the discrete coupling case resembles, for example, resilient mounted machinery, where each source contact is placed on a single resilient element. The fully connected case represents a more general coupling, for example a flange-like coupling between two components (with discretization by a finite series of point like DoFs).

For clarity all results will be presented for a single contact position (including translational and rotational DoFs).

4.2.1. Fully connected coupling

Let us first consider the fully connected coupling element (see Fig. 5a). The initial blocked force $\bar{\mathbf{f}}_{c_2}^{SI_1} \in \mathbb{C}^{12}$ is obtained using the inverse relation of Eq. (1) based on the mobility of the coupled *SIR* assembly. The initial forward transfer function $\mathbf{Y}_{rc_2}^{C_1} \in \mathbb{C}^{1\times12}$ is obtained from the same assembly. These are shown in grey in Figs. 7 and 8, respectively. Three plots are shown in each figure, corresponding to the blocked force (a) and the x/y blocked moments (b, c) in Fig. 7, and their associated transfer functions in Fig. 8. The same procedure is followed for the modified assembly, and the true blocked force and transfer functions are obtained. These are shown in orange in Figs. 7 and 8, respectively.

To illustrate the source/coupling impedance mismatch and the modification of the initial coupling element, a point mobility of the source, initial coupling and modified coupling are shown in Fig. 6a. Based on this modification, the exact, first and zeroth order CR-TPA equations (see Table 1) are used to predict the modified blocked force. These are shown in Fig. 7 in yellow, purple and green, respectively. Note that translational and rotational blocked forces are shown for a single contact only. Similar agreement is obtained for all other contacts.

As expected, the exact solution is in agreement with the true blocked force. The first and zeroth order approximations provide reasonable estimates of each blocked force, correctly predicting regions of both amplification and attenuation. Note

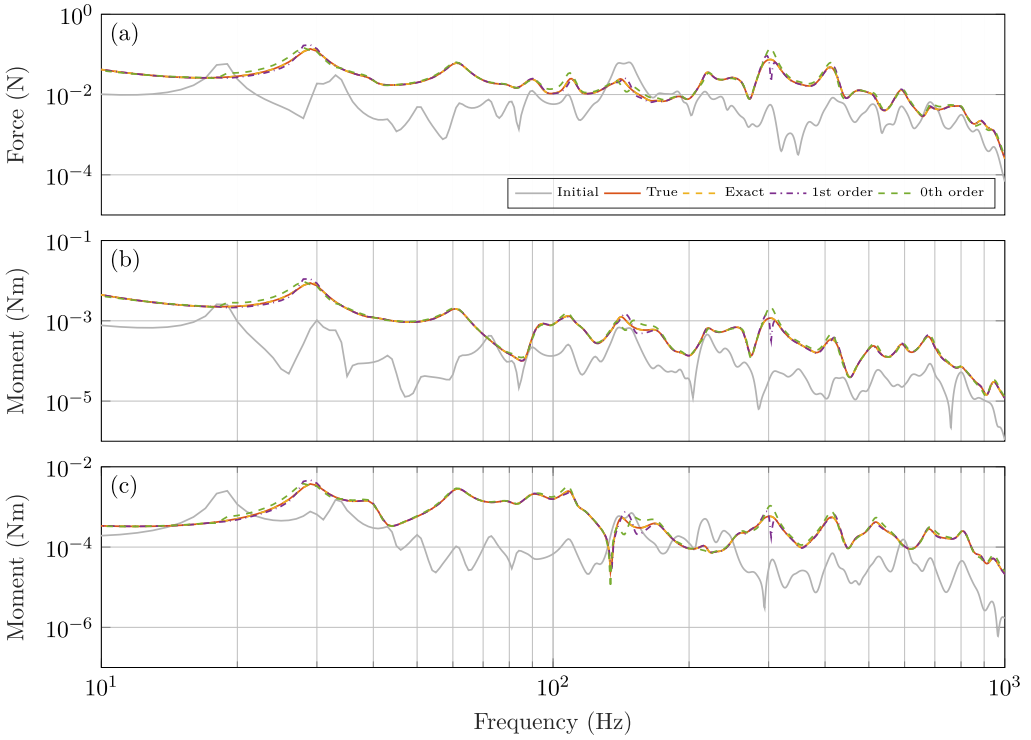

Fig. 7. Modified blocked force at the interface c_2 for a fully connected coupling (see Fig. 5a), obtained using the Component Replacement TPA approach and its approximations; (a) - blocked force, (b) - blocked x-moment, (c) - blocked y-moment. Grey plot corresponds to the blocked force obtained for the initial assembly. Remaining plots correspond to the new assembly with a component replacement.

that in this example the modification constitutes a stiffening of the coupling element, and so we generally see an increase in the blocked force, unlike the previous example where a softening was considered.

Based on the same modification as above, the exact, first and zeroth order CR-TPA equations are used to predict the modified forward transfer functions. These are shown in Fig. 8 in yellow, purple and grey, respectively. Note that the zeroth order approximation reduces to the identity matrix, and so the modified transfer function is the same as the initial transfer function.

As expected, the exact solution is in agreement with the true transfer function. The first order approximation provides a reasonable estimate of each transfer function, with a general improvement over the zeroth order (unmodified) estimate. As was observed in the previous example, it is clear from Figs. 7 and 8 that the modification of a constituent source component has a greater effect on the blocked force than the forward transfer function.

Having predicted the modified blocked force and forward transfer function we are able to make a target response prediction for the modified assembly. Shown in Fig. 9 are the target responses for the initial (grey) and modified (orange) assemblies. Also shown are the exact (yellow), first (purple) and zeroth (green) order CR-TPA predictions. As expected, the exact solution is in agreement with the true response. Both first and zeroth order approximations provide reasonable estimates of the response, particularly at higher frequencies where there is a greater impedance mismatch (see Fig. 6). Whilst the first order approximation generally provides better agreement, given its simplicity, the zeroth order approximation does a reasonable job predicting the effect of a component replacement.

4.2.2. Discrete coupling

The same procedure as above is now considered with the discrete coupling elements (see Fig. 5b) in place of the fully connected element. Note that each discrete coupling is nominally identical. A point mobility of the source (unchanged), initial coupling and modified coupling are shown in Fig. 6b. Note that the discrete coupling gives rise to a much greater dynamic range than the fully connected element.

The initial and modified blocked force and moment results are presented in Fig. 10. Similarly, the initial and modified forward transfer functions are presented in Fig. 11.

As expected, in both cases the exact solution is in agreement with the true blocked force/transfer function. The first and zeroth order approximations provide reasonable estimates, although some regions of greater error are observed (e.g. around 150 and 280 Hz), compared to the fully connected case. These errors likely arise due to the greater dynamic range of the discrete coupling element (see Fig. 6).

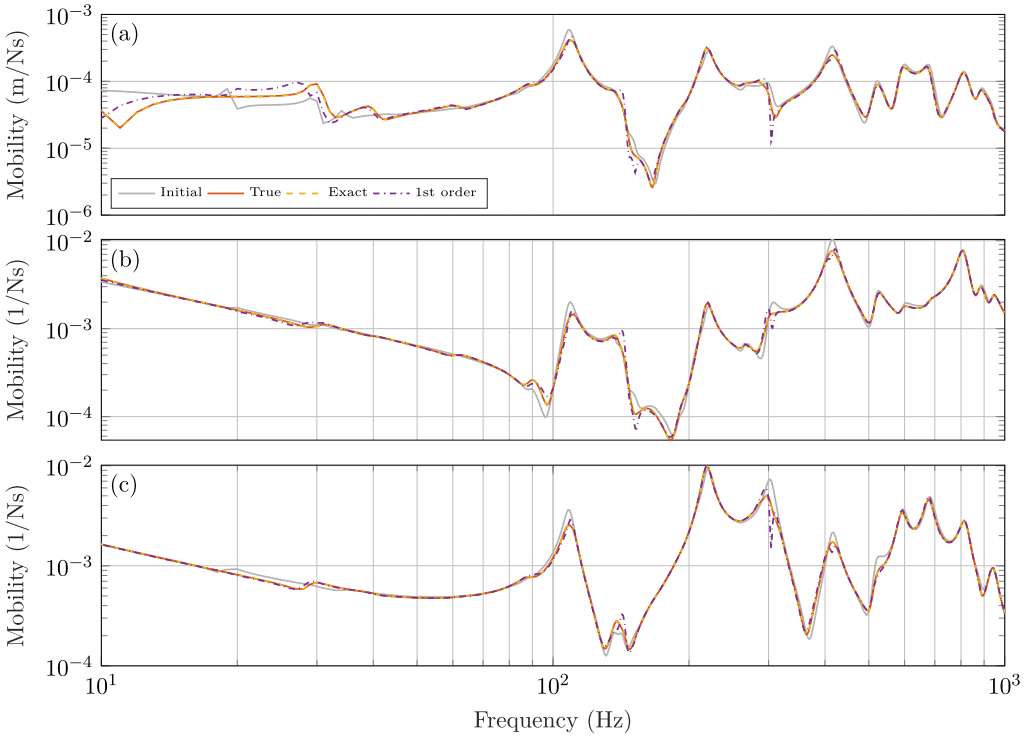

Fig. 8. Modified forward transfer function between the interface and target DoFs c_2 and r for a fully connected coupling (see Fig. 5a), obtained using the Component Replacement TPA approach and its approximations; (a) - force-velocity mobility, (b) - x-moment-velocity mobility, (c) - y-moment-velocity mobility. Grey plot corresponds to the transfer function obtained for the initial assembly. Remaining plots correspond to the new assembly with a component replacement.

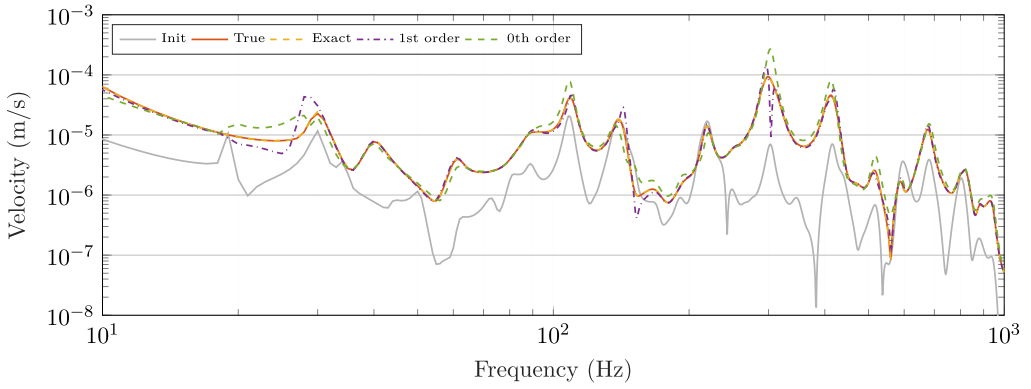

Fig. 9. Target response prediction using modified blocked force and forward transfer functions for a fully connected coupling (see Fig. 5a), obtained using the Component Replacement TPA approach and its approximations. Grey plot corresponds to the response obtained for the initial assembly. Remaining plots correspond to the new assembly with a component replacement.

The above errors are somewhat expected, given that the predictions were based on the assumption of a sufficient impedance mismatch between the source and coupling element (which may be violated in some regions due to the coupling element's greater dynamic range). Note that the over-predicted forward transfer function around 150 Hz is better estimated when the source contribution in the *SI* point impedance is retained, as in Eq. (42) (this result has been omitted for brevity). This is likely because the source is not sufficiently rigid to satisfy the assumption that $\tilde{\mathbf{Z}}^{SI}_{c_2c_2} \approx \mathbf{Z}^{I}_{c_2c_2}$. Nevertheless, we are typically more interested in the accuracy of a response prediction than the blocked force or transfer function individually.

Shown in Fig. 12 are the target responses for the initial (grey) and modified (orange) assemblies. Also shown are the exact (yellow), first (purple) and zeroth (green) order CR-TPA predictions. As expected, the exact solution is in agreement with the true response. Whilst the errors observed above are carried forward, the first and zeroth order approximations still provide reasonable estimates of the modified response. Again, the first order approximation generally provides better

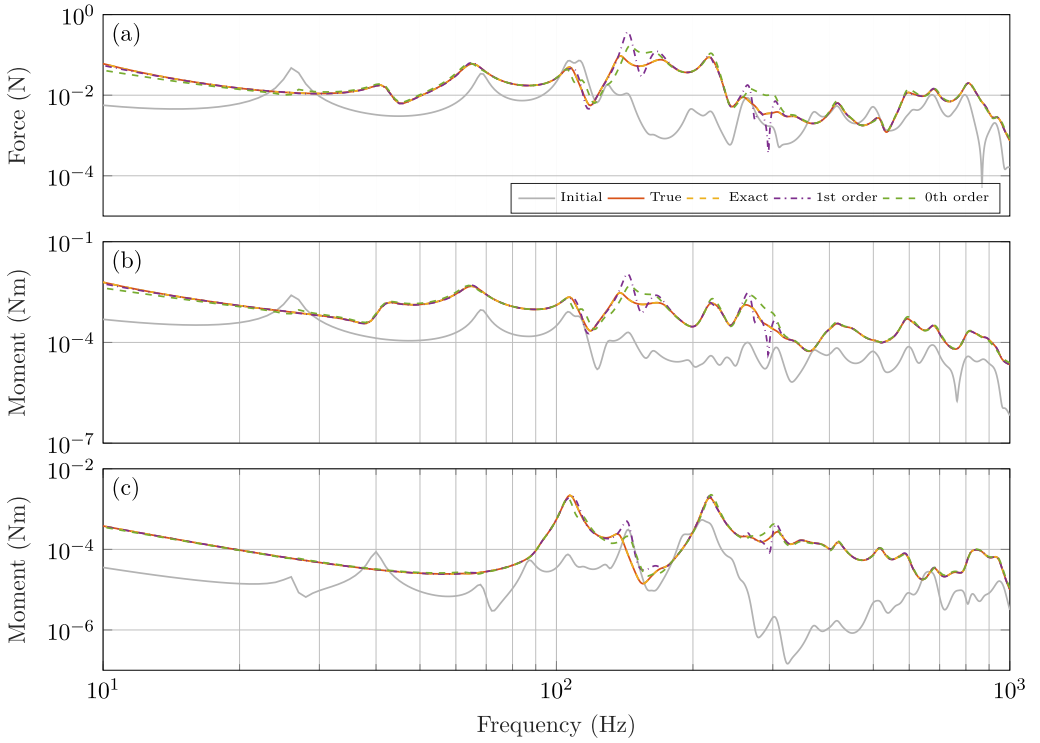

Fig. 10. Modified blocked force at the interface c_2 for discrete couplings (see Fig. 5b), obtained using the Component Replacement TPA approach and its approximations; (a) - blocked force, (b) - blocked x-moment, (c) - blocked y-moment. Grey plot corresponds to the blocked force obtained for the initial assembly. Remaining plots correspond to the new assembly with a component replacement.

agreement than the zeroth order. Nevertheless, given its simplicity the zeroth order approximation does a reasonable job predicting the effect of a component replacement.

4.2.3. Error analysis

The results presented above considered only a single initial and replacement coupling element, and so provide little information regarding the sensitivity of the CR-TPA approximations to their key assumption; an impedance mismatch between source and coupling element. In this section we will investigate the accuracy of the method for varying levels of a) the source/coupling impedance mismatch and b) the difference between initial and modified coupling elements. Given that the exact method is exact, only the first and zeroth order approximations will be considered here.

For ease of analysis, a single plate-like coupling element will be considered, corresponding to the fully connected element from Section 4.2.1. To investigate the sensitivity of the CR-TPA procedure, a combined error (including the blocked force and forward transfer function modification) is captured through a receiver response prediction,

$$v_r = \mathbf{Y}^{C}_{rc_2}\tilde{\mathbf{f}}^{Sl}_{c_2}. \tag{56}$$

From this, a dB error is calculated using,

$$\text{Error} = 20\left|\log_{10}\left(\frac{\langle|v_r^{mod}|\rangle}{\langle|v_r|\rangle}\right)\right| \tag{57}$$

where v_r^{mod} is the response prediction obtained as per CR-TPA, v_r is the true response, and $\langle\ \ \rangle$ represents an average across frequency.

To enable a reasonable comparison between different impedance mismatches, the fully connected element's mobility matrix (as used in Section 4.2.1) is artificially scaled to increase or decrease the mobility of initial and replacement coupling elements. Here, the initial coupling element mobility is given by,

$$\mathbf{Y}^{l_1} = \alpha\mathbf{Y}^{l} \tag{58}$$

where $\mathbf{Y}^{l}$ corresponds to the mobility of the initial element considered in Section 4.2.1, and α is a scaling parameter varied logarithmically between 10^2 and 10^{-2}. This scaling is intended to simulate both stiffer and more flexible coupling elements. The modified coupling element's mobility $\mathbf{Y}^{l_2}$ is determined by further scaling the initial mobility $\mathbf{Y}^{l_1}$,

$$\mathbf{Y}^{l_2} = \beta\mathbf{Y}^{l_1}. \tag{59}$$

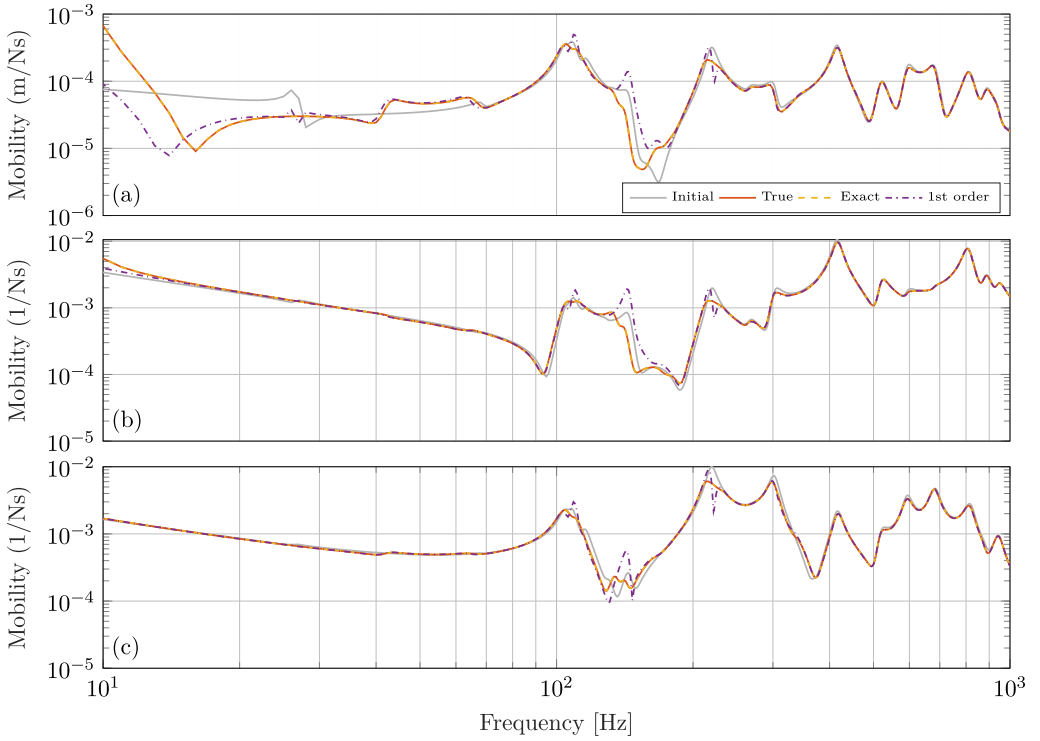

Fig. 11. Modified forward transfer function between the interface and target DoFs c_2 and r for discrete couplings (see Fig. 5b), obtained using the Component Replacement TPA approach and its approximations; (a) - force-velocity mobility, (b) - x-moment-velocity mobility, (c) - y-moment-velocity mobility. Grey plot corresponds to the transfer function obtained for the initial assembly. Remaining plots correspond to the new assembly with a component replacement.

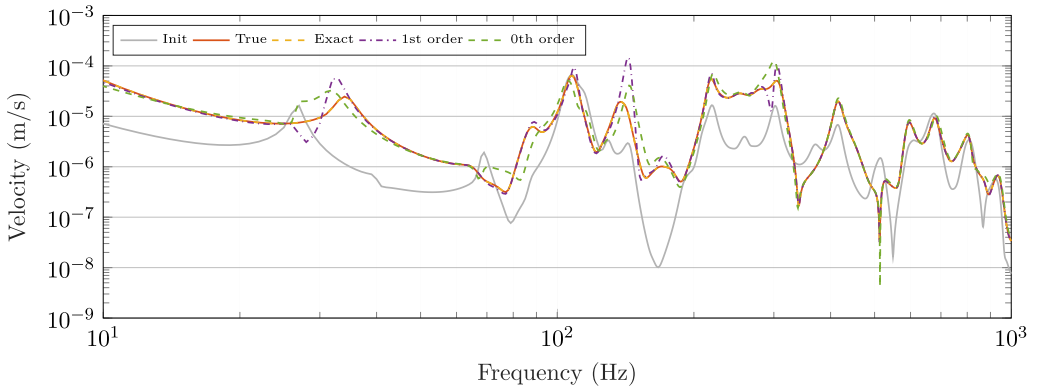

Fig. 12. Target response prediction using modified blocked force and forward transfer functions for discrete coupling case (see Fig. 5b), obtained using the Component Replacement TPA approach and its approximations. Grey plot corresponds to the response obtained for the initial assembly. Remaining plots correspond to the new assembly with a component replacement.

Here β is intended to simulate replacement coupling elements with different levels of flexibility/stiffness compared to the initial element $\mathbf{Y}^{I_1}$. β is varied logarithmically between 10 and 10^{-1}.

Shown in Fig. 13 are error plots corresponding to the first (a) and zeroth (b) order approximations. Note that the x-axis is defined as the ratio of frequency-averaged mobilities for the replacement and initial coupling elements, $x = \langle|Y^{I_2}|\rangle / \langle|Y^{I_1}|\rangle$, such that $x = 1$ indicates a modified element identical to the initial element. For $x < 1$ the modified element is stiffer than the initial, and for $x > 1$ the modified element is more flexible. The y-axis is defined as the ratio of frequency-averaged mobilities for the initial coupling element and source, $y = \langle|Y^{I_1}|\rangle / \langle|Y^{S}|\rangle$, such that $y = 1$ indicates an initial coupling element whose frequency-averaged mobility is the same as that of the source. Hence, for $y > 1$ the initial coupling element has a greater mobility than the source (i.e. is more flexible).

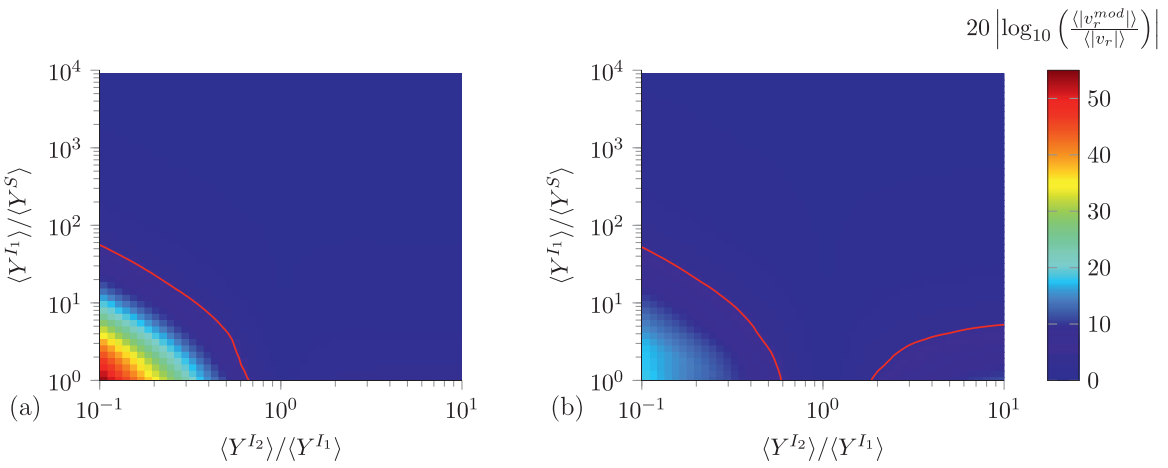

Fig. 13. Frequency-averaged dB error plots for the first (a) and zeroth (b) order approximations of a remote response with a fully connected coupling element. *x*-axis: relative modification $\langle Y^{I_2}\rangle/\langle Y^{I_1}\rangle$. *y*-axis: relative initial coupling/source mobility $\langle Y^{I_1}\rangle/\langle Y^S\rangle$. Colour: dB error $20\left|\log_{10}\left(\frac{\langle|v_r^{mod}|\rangle}{\langle|v_r|\rangle}\right)\right|$. Shown in red are the lines of constant 5dB error. (For interpretation of the references to color in this figure legend, the reader is referred to the web version of this article.)

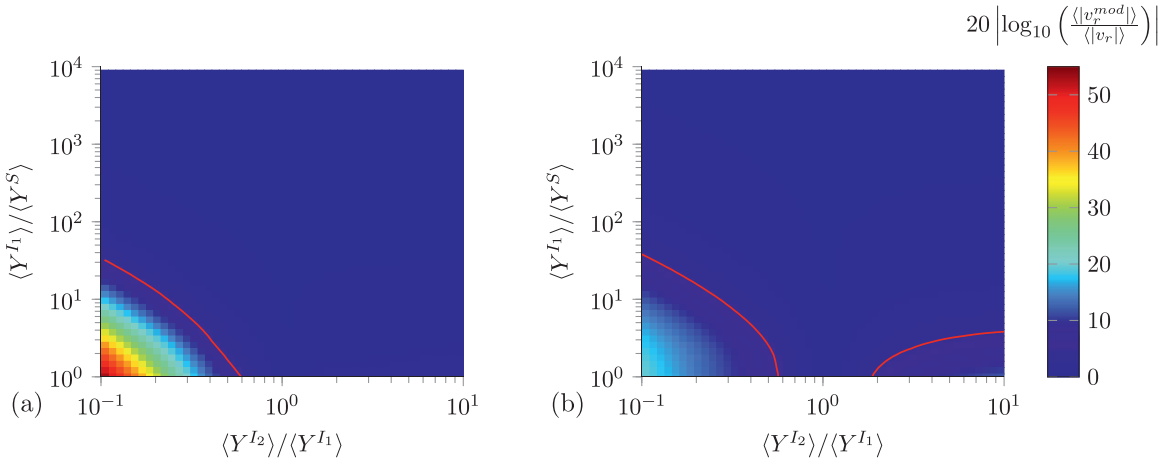

Fig. 14. Frequency-averaged dB error plots for the first (a) and zeroth (b) order approximations of a remote response with discrete coupling elements. *x*-axis: relative modification $\langle Y^{I_2}\rangle/\langle Y^{I_1}\rangle$. *y*-axis: relative initial coupling/source mobility $\langle Y^{I_1}\rangle/\langle Y^S\rangle$. Colour: dB error $20\left|\log_{10}\left(\frac{\langle|v_r^{mod}|\rangle}{\langle|v_r|\rangle}\right)\right|$. Shown in red are the lines of constant 5dB error. (For interpretation of the references to color in this figure legend, the reader is referred to the web version of this article.)

Consider the first order approximation. The error plot (Fig. 13a) indicates a maximum error when the initial coupling element's (frequency-averaged) mobility is equal to that of the source, and its replacement constitutes a stiffer element. This is expected, given that both of these conditions are at odds with the requirement of an impedance mismatch between source and coupling element. Interestingly, even with $\langle|Y^{I_1}|\rangle/\langle|Y^S|\rangle = 1$, providing the replacement coupling constitutes a more flexible element, the error remains below 5dB (indicated by the red contour). Given that one would typically be interested in reducing the transmission of vibration, replacement with a more resilient coupling is the more likely scenario in practice. In the presence of a greater impedance mismatch, $\langle|Y^{I_1}|\rangle/\langle|Y^S|\rangle \gtrsim 10^2$, an error less than 5dB is achieved for all replacement elements within $10^{\pm 1}$ of the initial element.

Now consider the zeroth order approximation. The error plot (Fig. 13b) indicates two regions of maximum error. These occur when the initial coupling element's (frequency-averaged) mobility is equal to that of the source and the replacement coupling differs significantly from the initial coupling, whether stiffer or more flexible. This error is expected as the zeroth order approximation is based on the assumption that $\mathbf{Z}^{I_1}_{c_1c_1} - \mathbf{Z}^{I_2}_{c_1c_1}$ is sufficiently small that it can be neglected in Eq. (31). Interestingly, for $\langle|Y^{I_1}|\rangle/\langle|Y^S|\rangle \approx 1$ the zeroth order error is much less sensitive than the first order error. This is expected given that $\mathbf{Z}^{I_1}_{c_1c_1} - \mathbf{Z}^{I_2}_{c_1c_1}$ in the first order approximation grows linearly as the difference between the initial and replacement coupling increases. Whilst valid for small values, the first order approximation 'over-shoots' the true inverse for large values (note that the second order term in the Taylor series expansion of a matrix inverse is opposite in sign to the first, so would

counteract this over-shoot). This term is neglected from the zeroth order approximation, so its error does not grow linearly with an increasing impedance difference.

To enable a reasonable comparison against an equivalent set of discrete elements (where the coupling mobility/impedance matrix has block diagonal structure) the fully connected element considered above is artificially 'decoupled' by setting all cross terms to 0, as in Eq. (55). This method was chosen over the explicit decoupling used in Section 4.2.2 as the resulting dynamics differed significantly from the fully connected element, as seen in Fig. 6. Although artificial, this decoupling will enable a direct comparison of the errors encountered between fully connected and discrete coupling elements.

Shown in Fig. 14 are the error plots corresponding to the first (a) and zeroth (b) order approximations for the discrete coupling case. Note that the general trend of the error is the same as in Fig. 13. This suggests that the accuracy of CR-TPA is not noticeably sensitive to cross-coupling between neighbouring contacts.

To put the above error analysis into a practical context, it is worth noting that in the automotive industry, for example, the body-to-isolator stiffness ratio K^B/K^I (which is equivalent to the source-coupling mismatch Y^I/Y^S) is designed to be as great as possible without compromising stability. Values of $K^B/K^I \sim Y^I/Y^S >> 10$ are typical.

5. Conclusions

Structural modification is a technique that can be used to investigate the effect of design changes made to an assembled structure. Its application has thus far been limited to the passive components that reside downstream of a defined source-receiver interface. Upstream structural modifications have been prohibited as they would alter the operational characteristics (i.e. blocked force) of the vibration source, and thus invalidate any response predictions made thereafter. The purpose of this paper has been to extend the possibility of structural modification upstream of the defined source-receiver interface, i.e. to simulate the replacement or modification of a sub-component within a source definition. To this end, we have introduced Component Replacement TPA (CR-TPA): a transmissibility-based structural modification method for in-situ transfer path analysis.

In contrast to component-based TPA, CR-TPA does not attempt to build an assembly out of individual components. Instead, it takes an assembled structure and considers the replacement of an individual component. In this way, CR-TPA may be viewed as an extension to in-situ TPA. One that enables upstream (also downstream, see Appendix A) structural modifications to be made.

At the heart of CR-TPA are the transmodification matrices that characterise the component replacement $I_1 \rightarrow I_2$. These matrices can be approximated to various degrees, and used to investigate the effect of different structural modifications. Equations are presented for exact, first, and zeroth order approximations. Based on a truncated Taylor series expansion, the first and zeroth order approximations are valid only in the presence of a resilient coupling (i.e. an impedance mismatch). A key result is that the zeroth order approximation requires only the transfer impedance of the initial and modified coupling elements. This information is readily available from experimental measurement or numerical modelling.

The CR-TPA method was validated numerically using coupled beam and plate simulations. It was shown that the blocked force, and to a lesser extent the forward transfer function, are both affected by the replacement of any coupling elements that reside within the source definition, and that the CR-TPA method is able to predict this change exactly. An error analysis based on coupled plate simulations suggests that when a first order approximation is used in the presence of a stiff coupling element, modifications should be restricted to replacement with a more resilient element. Also, when a sufficient impedance mismatch is achieved, both first and zeroth order approximations are seen to provide good estimates of the modified assembly, with frequency-averaged errors of less than 5dB.

Declaration of Competing Interest

The authors declare that they have no known competing financial interests or personal relationships that could have appeared to influence the work reported in this paper.

CRediT authorship contribution statement

J.W.R. Meggitt: Conceptualization, Methodology, Validation, Investigation, Writing - original draft, Writing - review & editing. **A.S. Elliott:** Writing - review & editing. **A.T. Moorhouse:** Writing - review & editing, Funding acquisition, Project administration. **A. Jalibert:** Resources. **G. Franks:** Resources.

Acknowledgement

This work was funded through the EPSRC Research Grant EP/P005489/1 Design by Science.

Appendix A. Downstream component replacement

Although not the primary concern of this paper, in what follows we will apply the developments above to the replacement of a sub-component within a receiver structure.

With reference to Fig. 1b, suppose the primary interface c_1 is accessible, and chosen as the interface where the blocked force is defined. We are interested in the replacement of the receiver sub-component $I_1 \rightarrow I_2$. Note that the blocked force $\bar{\mathbf{f}}^S_{c_1}$ is unaffected by this modification. Thus only a modification of the forward transfer function, $\mathbf{Y}^C_{rc_1}$, is required.

If there is measurement access to both the primary and secondary interfaces, a downstream component replacement can be achieved as follows. The primary interface blocked force $\bar{\mathbf{f}}^S_{c_1}$ can be propagated onto the secondary interface c_2 using a blocked force transmissibility (see Eq. (9)) corresponding to the modified assembly,

$$\bar{\mathbf{f}}^{SI_2}_{c_2} = -\mathbf{Z}^{I_2}_{c_2c_1}\left(\mathbf{Z}^S_{c_1c_1} + \mathbf{Z}^{I_2}_{c_1c_1}\right)^{-1}\bar{\mathbf{f}}^S_{c_1}. \tag{A.1}$$

Pre-multiplication by the modified forward transfer function, $\mathbf{Y}^{C_2}_{rc_2} = \mathbf{Y}^{C_1}_{rc_2}\mathbf{T}^{c_2\,(I_2\leftarrow I_1)}_{\mathbf{Y}}$, yields a response prediction in the modified assembly,

$$\mathbf{v}^{C_2}_r = \mathbf{Y}^{C_1}_{rc_2}\mathbf{T}^{c_2\,(I_2\leftarrow I_1)}_{\mathbf{Y}}\mathbf{Z}^{I_2}_{c_2c_1}\left(\mathbf{Z}^S_{c_1c_1} + \mathbf{Z}^{I_2}_{c_1c_1}\right)^{-1}\bar{\mathbf{f}}^S_{c_1} \tag{A.2}$$

where $\mathbf{T}^{c_2\,(I_2\leftarrow I_1)}_{\mathbf{Y}}$ is the transmodification matrix based on the secondary interface c_2 (see table 1).

Eq. (A.2) relates the primary interface blocked force to a remote receiver response in the modified assembly. Its matrix product must therefore correspond to the forward transfer function $\mathbf{Y}^{C_2}_{rc_1}$ in the modified assembly.

Finally, using the round trip identity [19],

$$\mathbf{Y}^C_{rc_2} = \mathbf{Y}^C_{rc_1}\left(\mathbf{Y}^C_{c_2c_1}\right)^{-1}\mathbf{Y}^C_{c_2c_2} \tag{A.3}$$

we can relate the initial and modified forward transfer functions using the equation,

$$\mathbf{Y}^{C_2}_{rc_1} = \mathbf{Y}^{C_1}_{rc_1}\mathbf{T}^{c_1\,(I_2\leftarrow I_1)}_{\mathbf{Y}} \tag{A.4}$$

where,

$$\mathbf{T}^{c_1\,(I_2\leftarrow I_1)}_{\mathbf{Y}} = \left(\mathbf{Y}^{C_1}_{c_2c_1}\right)^{-1}\mathbf{Y}^{C_1}_{c_2c_2}\mathbf{T}^{c_2\,(I_2\leftarrow I_1)}_{\mathbf{Y}}\mathbf{Z}^{I_2}_{c_2c_1}\left(\mathbf{Z}^S_{c_1c_1} + \mathbf{Z}^{I_2}_{c_1c_1}\right)^{-1} \tag{A.5}$$

is the transmodification matrix that transforms the forward transfer function from the primary interface in the initial assembly to that of the modified assembly.

When $\mathbf{T}^{c_2\,(I_2\leftarrow I_1)}_{\mathbf{Y}}$ is taken in its exact form Eq. (A.5) provides an exact modification of the assembly based on the properties of the initial assembly, the initial and modified coupling elements, and the initial and modified source-coupling assembly,

$$\mathbf{T}^{c_1\,(I_2\leftarrow I_1)}_{\mathbf{Y}} = \left(\mathbf{Y}^{C_1}_{c_2c_1}\right)^{-1}\left[\left(\mathbf{Y}^{C_1}_{c_2c_2}\right)^{-1} + \left(\mathbf{Z}^{SI_2}_{c_2c_2} - \mathbf{Z}^{SI_1}_{c_2c_2}\right)\right]^{-1}\mathbf{Z}^{I_2}_{c_2c_1}\left(\mathbf{Z}^S_{c_1c_1} + \mathbf{Z}^{I_2}_{c_1c_1}\right)^{-1}. \tag{A.6}$$

Note that the last bracketed term of Eq. (A.6) can be expressed equivalently as,

$$\left(\mathbf{Z}^S_{c_1c_1} + \mathbf{Z}^{I_2}_{c_1c_1}\right)^{-1} = \left(\mathbf{Z}^{SI_1}_{c_1c_1} + \left(\mathbf{Z}^{I_2}_{c_1c_1} - \mathbf{Z}^{I_1}_{c_1c_1}\right)\right)^{-1}. \tag{A.7}$$

As before, if the component I constitutes a resilient element, we can consider first and zeroth order approximations of the above. Depending on which form is taken, two first order approximations can be derived. Taking $\left(\mathbf{Z}^S_{c_1c_1} + \mathbf{Z}^{I_2}_{c_1c_1}\right)^{-1}$ and applying a first order Taylor expansion we obtain,

$$\mathbf{T}^{c_1\,(I_2\leftarrow I_1)}_{\mathbf{Y}} \approx \left(\mathbf{Y}^{C_1}_{c_2c_1}\right)^{-1}\mathbf{Y}^{C_1}_{c_2c_2}\left[\mathbf{I} - \left(\mathbf{Z}^{I_2}_{c_2c_2} - \mathbf{Z}^{I_1}_{c_2c_2}\right)\mathbf{Y}^{C_1}_{c_2c_2}\right]\mathbf{Z}^{I_2}_{c_2c_1}\mathbf{Y}^S_{c_1c_1}\left[\mathbf{I} - \mathbf{Z}^{I_2}_{c_1c_1}\mathbf{Y}^S_{c_1c_1}\right]. \tag{A.8}$$

Similarly, by taking $\left(\mathbf{Z}^{SI_1}_{c_1c_1} + \left(\mathbf{Z}^{I_2}_{c_1c_1} - \mathbf{Z}^{I_1}_{c_1c_1}\right)\right)^{-1}$ we obtain,

$$\mathbf{T}^{c_1\,(I_2\leftarrow I_1)}_{\mathbf{Y}} \approx \left(\mathbf{Y}^{C_1}_{c_2c_1}\right)^{-1}\mathbf{Y}^{C_1}_{c_2c_2}\left[\mathbf{I} - \left(\mathbf{Z}^{I_2}_{c_2c_2} - \mathbf{Z}^{I_1}_{c_2c_2}\right)\mathbf{Y}^{C_1}_{c_2c_2}\right]\mathbf{Z}^{I_2}_{c_2c_1}\left(\mathbf{Z}^{SI_1}_{c_1c_1}\right)^{-1}\left[\mathbf{I} - \left(\mathbf{Z}^{I_2}_{c_1c_1} - \mathbf{Z}^{I_1}_{c_1c_1}\right)\left(\mathbf{Z}^{SI_1}_{c_1c_1}\right)^{-1}\right]. \tag{A.9}$$

The principle difference between these two approximations is that the former requires the free source mobility $\mathbf{Y}^S_{c_1c_1}$, whilst the latter requires the coupled impedance term $\mathbf{Z}^{SI_1}_{c_1c_1}$. Note that this latter impedance term can be determined in-situ if measurements are performed at both the primary and secondary interface (see Eq. (20)). Given that both approximations require measurements at each interface, the latter is more convenient, as it avoids the need for the free mobility.

From the above we can identify the zeroth order approximations as,

$$\mathbf{T}^{c_1\,(I_2\leftarrow I_1)}_{\mathbf{Y}} \approx \left(\mathbf{Y}^{C_1}_{c_2c_1}\right)^{-1}\mathbf{Y}^{C_1}_{c_2c_2}\mathbf{Z}^{I_2}_{c_2c_1}\mathbf{Y}^S_{c_1c_1}. \tag{A.10}$$

or equivalently,

$$\mathbf{T}^{c_1\,(I_2\leftarrow I_1)}_{\mathbf{Y}} \approx \left(\mathbf{Y}^{C_1}_{c_2c_1}\right)^{-1}\mathbf{Y}^{C_1}_{c_2c_2}\mathbf{Z}^{I_2}_{c_2c_1}\left(\mathbf{Z}^{SI_1}_{c_1c_1}\right)^{-1}. \tag{A.11}$$

The downstream CR-TPA equations are summarised in Table A.4. Note that these CR-TPA equations provide an alternative approach to the dynamic sub-structuring procedures typically used in virtual prototyping and component-based simulation.

Table A4
Summary of downstream Component Replacement TPA equations for the modified forward transfer function.

Approximation	Modified transfer function: $\mathbf{Y}^{C_2}_{rc_1} = \mathbf{Y}^{C_1}_{rc_1}\mathbf{T}^{c_1\,(I_2 \leftarrow I_1)}_{\mathbf{Y}}$
Exact	$\mathbf{T}^{c_1}_{\mathbf{Y}} = \left(\mathbf{Y}^{C_1}_{c_2c_1}\right)^{-1}\left[\left(\mathbf{Y}^{C_1}_{c_2c_2}\right)^{-1} + \left(\mathbf{Z}^{SI_2}_{c_2c_2} - \mathbf{Z}^{SI_1}_{c_2c_2}\right)\right]^{-1}\mathbf{Z}^{I_2}_{c_2c_1}\left(\left(\mathbf{Y}^{S}_{c_1c_1}\right)^{-1} + \mathbf{Z}^{I_2}_{c_1c_1}\right)^{-1}$
	$\mathbf{T}^{c_1}_{\mathbf{Y}} = \left(\mathbf{Y}^{C_1}_{c_2c_1}\right)^{-1}\left[\left(\mathbf{Y}^{C_1}_{c_2c_2}\right)^{-1} + \left(\mathbf{Z}^{SI_2}_{c_2c_2} - \mathbf{Z}^{SI_1}_{c_2c_2}\right)\right]^{-1}\mathbf{Z}^{I_2}_{c_2c_1}\left(\mathbf{Z}^{SI_1}_{c_1c_1} + \left(\mathbf{Z}^{I_2}_{c_1c_1} - \mathbf{Z}^{I_1}_{c_1c_1}\right)\right)^{-1}$
First order	$\mathbf{T}^{c_1}_{\mathbf{Y}} \approx \left(\mathbf{Y}^{C_1}_{c_2c_1}\right)^{-1}\mathbf{Y}^{C_1}_{c_2c_2}\left[\mathbf{I} - \left(\mathbf{Z}^{I_2}_{c_2c_2} - \mathbf{Z}^{I_1}_{c_2c_2}\right)\mathbf{Y}^{C_1}_{c_2c_2}\right]\mathbf{Z}^{I_2}_{c_2c_1}\mathbf{Y}^{S}_{c_1c_1}\left[\mathbf{I} - \mathbf{Z}^{I_2}_{c_1c_1}\mathbf{Y}^{S}_{c_1c_1}\right]$
	$\mathbf{T}^{c_1}_{\mathbf{Y}} \approx \left(\mathbf{Y}^{C_1}_{c_2c_1}\right)^{-1}\mathbf{Y}^{C_1}_{c_2c_2}\left[\mathbf{I} - \left(\mathbf{Z}^{I_2}_{c_2c_2} - \mathbf{Z}^{I_1}_{c_2c_2}\right)\mathbf{Y}^{C_1}_{c_2c_2}\right]\mathbf{Z}^{I_2}_{c_2c_1}\left(\mathbf{Z}^{SI_1}_{c_1c_1}\right)^{-1}\left[\mathbf{I} - \left(\mathbf{Z}^{I_2}_{c_1c_1} - \mathbf{Z}^{I_1}_{c_1c_1}\right)\left(\mathbf{Z}^{SI_1}_{c_1c_1}\right)^{-1}\right]$
Zeroth order	$\mathbf{T}^{c_1}_{\mathbf{Y}} \approx \left(\mathbf{Y}^{C_1}_{c_2c_1}\right)^{-1}\mathbf{Y}^{C_1}_{c_2c_2}\mathbf{Z}^{I_2}_{c_2c_1}\mathbf{Y}^{S}_{c_1c_1}$
	$\mathbf{T}^{c_1}_{\mathbf{Y}} \approx \left(\mathbf{Y}^{C_1}_{c_2c_1}\right)^{-1}\mathbf{Y}^{C_1}_{c_2c_2}\mathbf{Z}^{I_2}_{c_2c_1}\left(\mathbf{Z}^{SI_1}_{c_1c_1}\right)^{-1}$

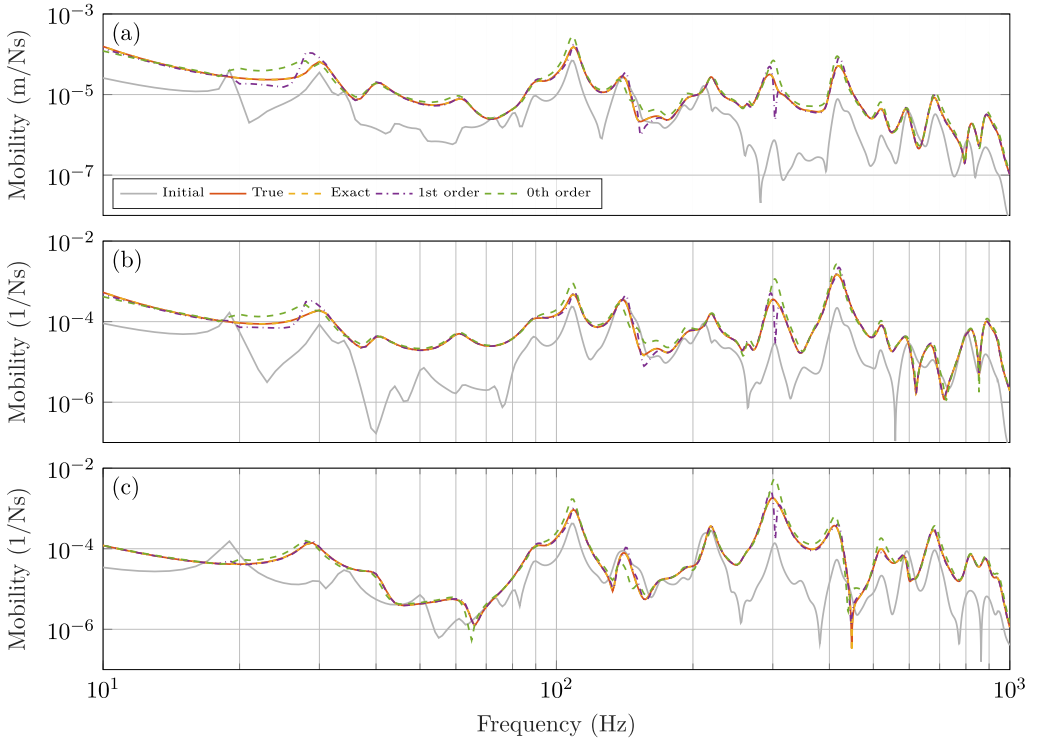

Fig. A14. Modified forward transfer function between the primary interface and target DoFs c_1 and r for a continuous coupling (see Fig. 5a), obtained using the Component Replacement TPA approach and its approximations; (a) - force-velocity mobility, (b) - x-moment-velocity mobility, (c) - y-moment-velocity mobility. Grey plot corresponds to the transfer function obtained for the initial assembly. Remaining plots correspond to the new assembly with a component replacement.

Whilst they are limited to the modification $I_1 \rightarrow I_2$, in the presence of a resilient suspension they yield simplified forms (see Eqs. (A.9) and (A.11)) which avoid the need to measure the free interface properties of source and receiver, instead relying on in-situ measurements. This may prove more useful in practical TPA applications where coupling element replacements are of interest.

The downstream CR-TPA equations presented in Table A.4 have been applied to the case study presented in Section 4.2 for the fully connected coupling (see Fig. 5a). Shown in Fig. A.14 are the initial (grey), true (orange) and modified forward transfer functions $\mathbf{Y}^{C_2}_{rc_1}$, based on the exact (yellow), first (purple) and zeroth (green) order approximations. As expected, the exact solution is in agreement with the forward transfer function. The first and zeroth order approximations also provide reasonable estimates, the zeroth order in particular given its simplicity.

References

[1] M. van der Seijs, D. de Klerk, D. Rixen, General framework for transfer path analysis: history, theory and classification of techniques, Mech. Syst. Signal Process. 68-69 (2016) 217–244.
[2] A. Oktav, Y. Çetin, A. Günay, Transfer path analysis: current practice, trade-offs and consideration of damping, Mech. Syst. Signal Process. 85 (2017) 760–772.
[3] J. Verheij, Multi-path sound transfer from resiliently mounted shipboard machinery, Technisch Physische Dienst TNO-TH, 1982 Ph.D. thesis.

[4] A. Elliott, A. Moorhouse, T. Huntley, S. Tate, In-situ source path contribution analysis of structure borne road noise, J. Sound Vibr. 332 (24) (2013) 6276–6295.
[5] D. de Klerk, D. Rixen, Component transfer path analysis method with compensation for test bench dynamics, Mech. Syst. Signal Process. 24 (6) (2010) 1693–1710.
[6] D. de Klerk, A. Ossipov, Operational transfer path analysis: theory, guidelines and tire noise application, Mech. Syst. Signal Process. 24 (7) (2010) 1950–1962.
[7] K. Janssens, P. Gajdatsy, L. Gielen, P. Mas, L. Britte, W. Desmet, H. Van Der Auweraer, OPAX: a new transfer path analysis method based on parametric load models, Mech. Syst. Signal Process. 25 (4) (2011) 1321–1338.
[8] P. Gajdatsy, K. Janssens, W. Desmet, H. Van Der Auweraer, Application of the transmissibility concept in transfer path analysis, Mech. Syst. Signal Process. 24 (7) (2010) 1963–1976.
[9] O. Guasch, C. García, J. Jové, P. Artís, Experimental validation of the direct transmissibility approach to classical transfer path analysis on a mechanical setup, Mech. Syst. Signal Process. 37 (1–2) (2013) 353–369.
[10] A. Elliott, N. Sanei, M. Glesser, Combining structural modification with in-situ transfer path analysis to solve nose and vibration problems, in: Proceedings of 23rd International Congress on Acoustics, ICA 2019, Aachen, Germany, 2019, pp. 427–434.
[11] M. Haeussler, D. Kobus, D. Rixen, Parametric design optimization of e-compressor NVH using blocked forces and substructuring, Mech. Syst. Signal Process. 150 (107217) (2021).
[12] P. Wagner, P. Hülsmann, M. Van Der Seijs, Application of dynamic substructuring in NVH design of electric drivetrains, in: 29th International Conference on Noise and Vibration Engineering, ISMA 2020 and 8th International Conference on Uncertainty in Structural Dynamics, USD, Leuven (Online), 2020.
[13] A. Moorhouse, A. Elliott, T. Evans, In situ measurement of the blocked force of structure-borne sound sources, J. Sound Vibr. 325 (4–5) (2009) 679–685.
[14] Y. Bobrovnitskii, A theorem on representation of the field of forced vibrations of a composite elastic system, Acoust. Phys. 47 (5) (2001) 507–510.
[15] J. Meggitt, On in-situ methodologies for the characterisation and simulation of vibro-acoustic assemblies, University of Salford, 2017 Ph.D. thesis.
[16] A. Hjørungnes, Complex-Valued Matrix Derivatives, vol. 369, first ed., Cambridge University Press, New York, 2013.
[17] N. Maia, A. V. Urgueira, R. Almei, Whys and wherefores of transmissibility, Vibration Analysis and Control - New Trends and Developments, Intechopen, 2011.
[18] J. Meggitt, A. Elliott, A. Moorhouse, A. Jalibert, G. Franks, Component replacement transfer path analysis, in: 29th International Conference on Noise and Vibration Engineering, ISMA 2020 and 8th International Conference on Uncertainty in Structural Dynamics, USD, Leuven (Online), 2020.
[19] A. Moorhouse, T. Evans, A. Elliott, Some relationships for coupled structures and their application to measurement of structural dynamic properties in situ, Mech. Syst. Signal Process. 25 (5) (2011) 1574–1584.